Dealing with allometry in linear and geometric morphometrics: a taxonomic case study in the *Leporinus cylindriformis* group (Characiformes: Anostomidae) with description of a new species from Suriname

BRIAN L SIDLAUSKAS[1,2,3,*], JAN H. MOL[4] and RICHARD P. VARI FLS[3]

[1]*Oregon State University, Department of Fisheries and Wildlife, 104 Nash Hall, Corvallis, OR 97331-3803, USA*
[2]*National Evolutionary Synthesis Center, 2024 W. Main St. A200, Durham, NC 27705, USA*
[3]*Department of Vertebrate Zoology, MRC-159, National Museum of Natural History, PO Box 37012, Smithsonian Institution, Washington, DC 20013-7012, USA*
[4]*Department of Biology & Center for Agricultural Research in Suriname, Anton de Kom University of Suriname, PO Box 9212, CELOS-Building, University Campus, Leysweg, Paramaribo, Suriname*

To achieve maximum efficacy, taxonomic studies that seek to distinguish amongst species must first account for allometric shape variation within species. Two recently developed software packages (SMATR and MorphoJ) offer regression-based allometric approaches that are notable for their statistical power and ease of use and that may prove highly useful to taxonomists working with linear or geometric morphometric data. We investigate species delimitation of the slender-bodied fishes in the *Leporinus cylindriformis* group using these programs and demonstrate the utility of the allometric corrections that they provide. Without allometric correction, many pairs of species are difficult to distinguish on the basis of morphometrics, but once regressions are used to account for marked allometric variation within species, most of the recognized species in this group can be readily distinguished with linear or geometric morphometrics, particularly using variation in the depth of the body. Both approaches returned congruent patterns of separation amongst putative species, but the geometric approach in MorphoJ distinguished amongst four more pairs of species than did the linear approach in SMATR and appears to provide slightly more statistical power. Based on distinctive morphometrics, meristics, and coloration, a highly elongate species of *Leporinus* from the Suriname, Corantijn, and Coppename rivers of Suriname is described herein as a new species, **Leporinus apollo sp. nov.** The unique *L. cylindriformis* holotype from Porto de Moz, Brazil differs in morphology, meristics, and pigmentation from specimens commonly referred to that species from the main basin of the Amazon; the latter specimens may represent an additional undescribed species. The *L. cylindriformis* holotype itself may represent a rare species or a specimen collected at the edge of its native range. Measurements of the holotype and paratype of *Leporinus niceforoi*, which were collected in the Amazonian slope of Colombia, differ substantially from similarly pigmented and putatively conspecific specimens from Amazonian portions of Ecuador and Peru. Recently collected specimens from Colombia are needed to determine whether the observed morphometric variation encompassed by the current concept of *L. niceforoi* indicates a morphocline within a single species, suggests the presence of multiple cryptic species, or results from shrinkage of the types. In all these cases, linear or geometric morphometric data can reliably differentiate amongst species, but only after one accounts for allometric shape variation. The new SMATR and MorphoJ software packages both offer easy and effective approaches to such allometrically informed taxonomy, and may prove useful to any systematist working on taxa that change shape as they grow.

*Corresponding author. E-mail: brian.sidlauskas@oregonstate.edu

INTRODUCTION

Morphometrics and meristics have served as primary methods of species discrimination throughout the history of ichthyology. Eighteenth and early 19th century works frequently detailed differences in counts (Bloch, 1794; Cuvier, 1816) and measured differences amongst species became part of standard practice by the mid 19th century (Müller & Troschel, 1845, 1848, 1849; Cuvier & Valenciennes, 1850; Günther, 1864) By the mid 20th century, a detailed system of standard linear measurements had been codified (Hubbs & Lagler, 1958, 2004). Differences amongst species were (and still are) explored commonly by comparing means and ranges of raw measures or ratios of these measures in head or standard length (e.g. Hubbs & Bailey, 1940), with bivariate regression often used to control for ontogenetic variation (Teissier, 1936; Morton & Miller, 1954; Marr, 1955; Miller, 1963; Gould, 1971; Turner, Pitcher & Grimm, 1989; Fink, 1993). As morphometric datasets can include dozens of variables, multivariate techniques like principal components analysis (PCA; Jolicoeur, 1963) that can summarize many variables on a single axis also became common practice in the analysis of linear measurements.

The field of morphometrics underwent a revolution in the 1980s and 1990s with the advent of image-based, geometric methods that analyse variation in coordinate systems (Bookstein *et al*., 1985; Bookstein, 1991; Rohlf, 1993; Rohlf & Marcus, 1993; Dryden & Mardia, 1998; Adams, Rohlf & Slice, 2004; Sheets, 2004). Advocates of geometric analysis claim several benefits, including greater statistical power and improved ease of visualization (Rohlf & Marcus, 1993). Although the initial analysis of landmark data requires manipulations that linear data do not, such as a control for the effects of scaling, rotation, and translation (Rohlf & Slice, 1990) and the projection of data from a curved shape space into its linear analogue (Rohlf, 1996), the principles of the eventual multivariate analysis of traditional and geometric datasets are similar. Standard statistical techniques including PCA, regression, and analysis of variance (ANOVA) can be applied to geometric and traditional data alike.

All of the above methods, from simple comparison of mean ratios and their standard deviations to sophisticated statistical analyses of landmark configurations are used currently in studies of taxonomy and population structure. Most studies, however, employ only one method, and empirical comparisons amongst methods have been uncommon (see however Birch, 1997; Fink & Zelditch, 1997; Parsons, Robinson & Hrbek, 2003; Maderbacher

et al., 2008). This case study explicitly compares the performance of linear and geometric morphometrics in discriminating amongst the same set of specimens and finds that, in at least this case, both are highly effective at discriminating nominal species once allometric variation within species is accounted for properly.

Although some studies correct for the influence of allometric shape variation within species on effective discrimination amongst species using sheared PCA, regression, or analysis of covariance (Bookstein *et al*., 1985; Fink & Zelditch, 1995; Chernoff & Machado-Allison, 1999; Rincon, 2000; Fernandes *et al*., 2002; Parsons *et al*., 2003; Chernoff & Machado-Allison, 2005; Sidlauskas, Chernoff & Machado-Allison, 2006), many do not. When such corrections are not employed, analysis may fail to realise the full potential of a morphometric dataset and more problematically, may conflate differences in shape because of differences in the size of the available specimens with true shape differences amongst species. This contribution examines the degree to which the regression-based approaches to allometry in the relatively new programs SMATR (Warton *et al*., 2006) and MorphoJ (Klingenberg, 2008) improve the ability to separate nominal species in the *Leporinus cylindriformis* group (an enigmatic complex of South American freshwater fishes) on the basis of morphometrics. As is common in studies of museum specimens, the available samples of each nominal species differ substantially in mean, minimum, and maximum size. We find that either of these two new methods for allometric correction offers an easily accessible way to draw meaningful comparisons amongst such samples, and that the explicit attention to allometry improves the power of the comparisons dramatically.

Within the species-rich and geographically widespread characiform fish genus *Leporinus* (family Anostomidae), the *L. cylindriformis* group is a cluster of elongate species possessing a series of dark spots centred along the lateral line. The central species in this assemblage, *L. cylindriformis*, was described by Borodin (1929) based upon a single holotype (Fig. 1) collected at Porto de Moz, Brazil, and a series of notes and illustrations prepared by Louis Agassiz of the Harvard Museum of Comparative Zoology shortly before his death. In later years, several similar species were discovered throughout central and northern South America, including the more highly patterned *Leporinus niceforoi*, described from the Colombian Amazon (Fowler, 1943). Populations referred to *L. niceforoi* were later reported from Amazonian Peru and Ecuador. Description of species of the *L. cylindriformis* group continued with *Leporinus klausewitzi* from the Amazon River near Manaus,

Brazil (Géry, 1960), and *Leporinus ortomaculatus* from the Orinoco and Negro river basins (Garavello, 2000). The *L. cylindriformis* group recently attracted additional taxonomic interest with the description of *Leporinus amazonicus* from the vicinity of Manaus, Brazil (Santos & Zuanon, 2008) in a study that cited an extensive series of *L. cylindriformis* amongst the materials examined (see Fig. 2 for a specimen from the same series) albeit not the holotype of the species.

During an ichthyological survey of the Coppename River, Suriname, a single enigmatic specimen of an elongate *Leporinus* (Fig. 3) was discovered and tentatively referred to an undescribed species similar to *L. cylindriformis* (Willink & Sidlauskas, 2006). However, the original illustration of the *L. cylindriformis* type shows an individual with three narrow, horizontally elongate dark spots centred along the lateral line but no other markings, whereas the specimen from Suriname possesses a large fourth spot along the lateral line, distinct bars across the dorsal surface of the body, and several additional series of dark spots reminiscent of, but not identical to, the colour pattern of *L. niceforoi*. The subsequent collection of a larger series of this possibly new species from the Corantijn and Suriname Rivers, including juveniles (Fig. 4), and the discovery of a lot of similar specimens in the National Museum of Natural History prompted us to initiate a thorough comparison of the putatively new species with the holotype of *L. cylindriformis* and similar species in South America. In addition to confirming the novelty of the Suriname material, this analysis provided an excellent opportunity to test the relative power of allometrically informed linear and geometric morphometrics to distinguish amongst the nominal species in the *L. cylindriformis* group and to identify potentially new species.

This study had three major objectives:

1. To evaluate and contrast the ability of linear and geometric morphometrics to distinguish amongst nominal species after allometric corrections have accounted for ontogenetic shape variation within nominal species, using the *L. cylindriformis* complex as a case study.
2. To determine whether the enigmatic samples of *Leporinus* recently collected in Suriname match a previously recognized species or represent an undescribed species.
3. To compare the type material of the earliest described species in this group (*L. cylindriformis* and *L. niceforoi*) with putative conspecifics, and to determine whether those names are being correctly applied.

MATERIAL AND METHODS

The list of examined specimens (Appendix) includes examples of all described *Leporinus* species that closely match the *L. cylindriformis* holotype or the material from Suriname in morphometrics and pigmentation. All specimens are alcohol preserved except those marked as cleared-and-stained (CS), which were prepared according to Taylor & Van Dyke (1985). Institutional abbreviations are as listed at http://www.asih.org/node/204 (Sabaj Pérez, 2010), with the addition of NZCS, the National Zoological Collection of Suriname, Anton de Kom University, Paramaribo. Other distinctly elongate species of *Leporinus* possessing colour patterns that differed from those of the species in the *L. cylindriformis* complex were excluded from the analysis. For example, both *Leporinus brunneus* and *Leporinus nigrotaeniatus* are very slender but possess a dark midlateral stripe on the body that easily separates them from members of the *L. cylindriformis* group. Most of the many species in the *Leporinus friderici* complex possess a spotted colour pattern reminiscent of that in *L. cylindriformis*, but also have obviously deeper bodies. *Leporinus friderici* and the similar *L. lebaili* were included for comparative purposes and to demonstrate the clear morphometric differences between the *L. cylindriformis* complex and the *L. friderici* complex, but no effort was made to sample comprehensively the dozens of species allied to *L. friderici*.

Prior taxonomy, pigmentation, geography, and meristics were used to identify ten *a priori* groups representing potentially distinct species. These *a priori* designations were intended to separate out any potentially distinct groupings of specimens for the purposes of morphological analysis. Although these groupings follow the most current taxonomy, it is worth mentioning that these groups represent an underlying morphological species concept and do not explicitly address the genetic, reproductive, or phylogenetic divisions that could help determine the biological reality of these nominal species. Nevertheless, the morphospecies approach provides the only way to analyse historical specimens for which DNA is not available, such as the critically important type specimens. The *a priori* groups included seven previously described species: *Leporinus amazonicus*, *L. cylindriformis*, *L. friderici*, *L. klausewitzi*, *L. lebaili*, *L. niceforoi*, and *L. ortomaculatus*. Nontype specimens assigned to *L. niceforoi* and *L. cylindriformis* were treated as a putative separate species and appear throughout as *L.* cf. *niceforoi* and *Leporinus* sp., respectively. The elongate specimens from the Suriname, Corantijn, and Coppename rivers of Suriname comprised the tenth *a priori* group and were found in the course of analysis to represent a distinct species.
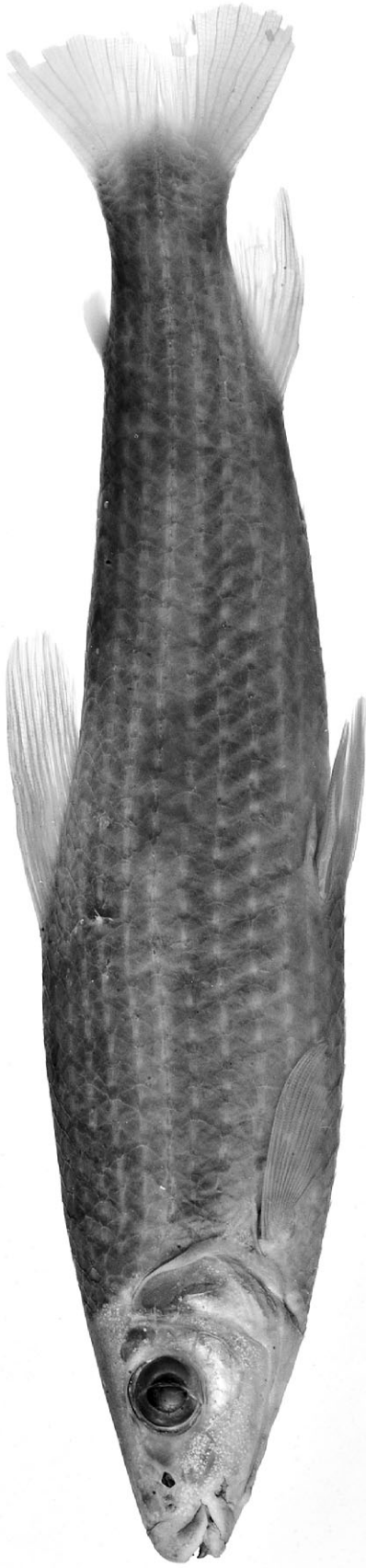
Figure 1. *Leporinus cylindriformis*, MCZ 20430, holotype, 188.0 mm standard length; Brazil, Pará, Rio Xingu at Porto de Moz. Image © President and Fellows of Harvard College.
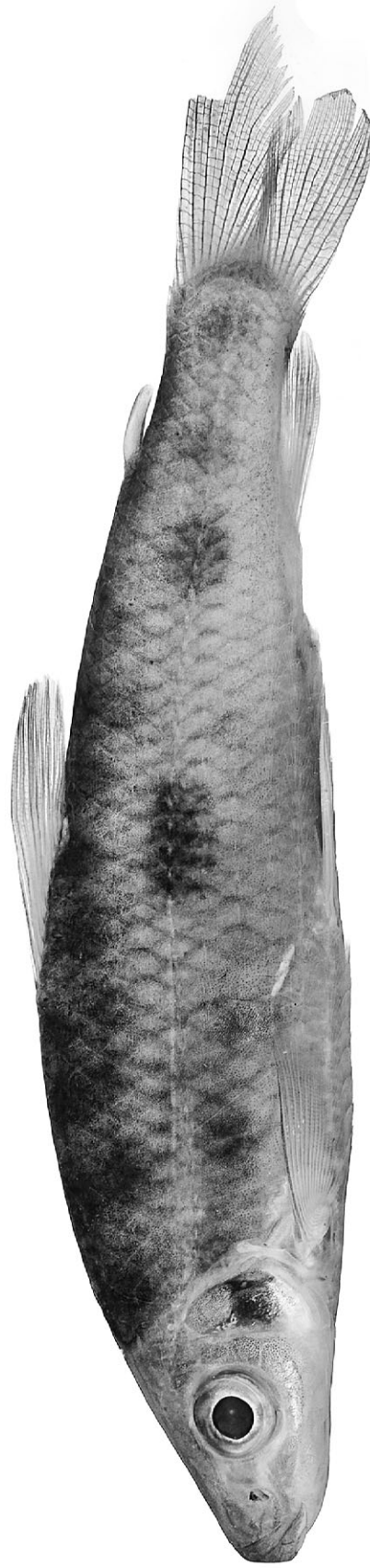
Figure 2. *Leporinus* sp., INPA 15405, 115.9 mm standard length; Brazil, Rondônia, Rio Ucupá at Ji Parana. Right of specimen photographed with image reversed to place head at left. Previously considered conspecific with *Leporinus cylindriformis*.

Figure 3. *Leporinus apollo* **sp. nov.**, FMNH 116827, holotype, 111.1 mm standard length; Suriname, Saramacca, Coppename River, Sidonkrutu, sand island and channel.

Figure 4. *Leporinus apollo* **sp. nov.**, MHNG 2673.002, paratype, 48.6 mm standard length; Suriname, Corantijn River, Kaw Falls (04°59′48.3″N, 57°37′49.5″W).

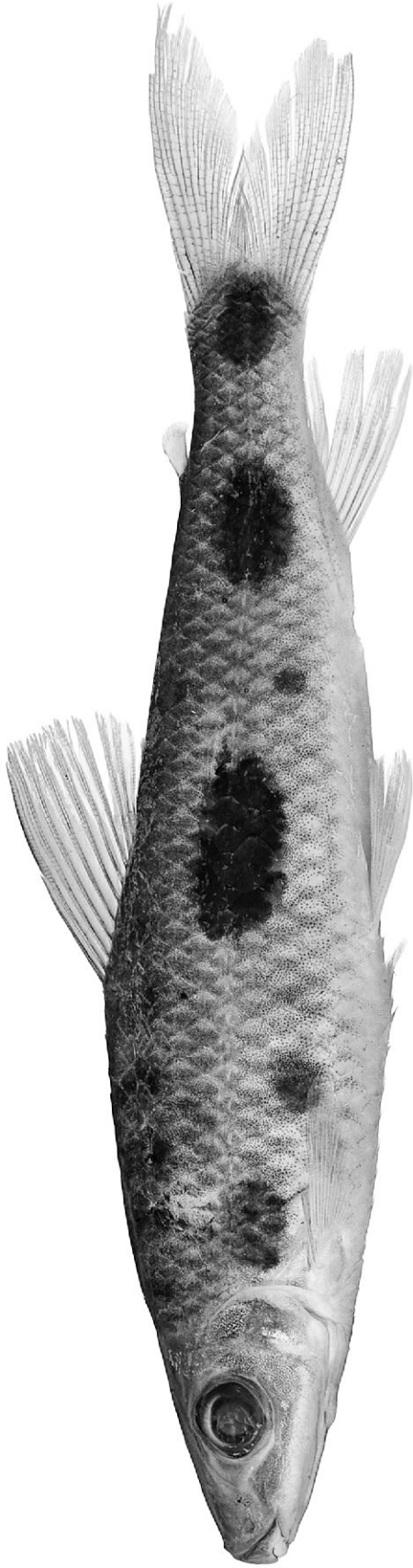That species appears throughout the remainder of the text as *Leporinus apollo*, the name given to it in its formal description in the Discussion section.

TRADITIONAL MORPHOMETRICS

All measurements reported in lists of material examined are standard lengths (SLs), taken from the tip of the upper jaw to the anterior limit of the hypural plate as identified by left–right manipulation of the caudal fin. This definition of standard length parallels our choice of the most reliable geometric landmark in this region (see Fig. 5 and its explanation below) and incorporates (to the degree possible) the same information in the linear and geometric datasets. Digital callipers were used to take 37 additional point-to-point measurements from the left side of each specimen. Of these, 18 follow Sidlauskas, Garavello & Jellen (2007) who slightly modified the method proposed by Winterbottom (1980). The remaining 19 measures were added to produce a more complete truss network (Bookstein *et al*., 1985). These 37 measurements were converted to their base 10 logarithms to linearize allometries (Huxley, 1932) and roughly equalize variances (Jolicoeur, 1963) and then subjected to PCA using the covariance matrix as implemented in PAST (Hammer, Harper & Ryan, 2001). The linear and geometric datasets (see below) are freely available from Dryad (http://dx.doi.org/10.5061/dryad.8151).

We expected that at least one principal component would describe allometric scaling, as identified by a significant product-moment correlation with log SL

and non-equivalence of principal component loadings for the various measures (Jolicoeur, 1963). Purely isometric scaling vectors have identical loadings for each measure (Jolicoeur, 1963), but these are rare in biological systems. We tested for difference amongst species on such size-correlated shape axes by comparing the slopes and elevations of reduced-major axis (RMA) regression lines via the slope.com and elev.com routines in the SMATR package of R (Warton *et al*., 2006). These significance tests were adjusted with a sequential Bonferroni correction (Rice, 1989) at a table-wide alpha level of 0.05. Essentially, this method compares the characteristic regression line of each *a priori* group and can identify differences in overall allometric trajectories even when the available specimens differ greatly in size amongst groups. RMA regression was chosen over ordinary regression because it summarizes a symmetrical geometric relationship between the variables in which results are unchanged if the *x* and *y* axes are exchanged (Warton *et al*., 2006), rather than describing a predictive relationship between the variables. RMA regression is preferred generally over least squares regression in studies when determination of the equation of the line of fit is of primary interest rather than demonstration of a relationship between the variables, as it is in studies of allometry (Harvey & Pagel, 1991; Nunn & Barton, 2000; Warton *et al*., 2006; Kimmel, Sidlauskas & Clack, 2009).

Amongst-species structure on eigenvectors from the PCA not correlated with standard length (non-allometric eigenvectors) was analysed with one-way
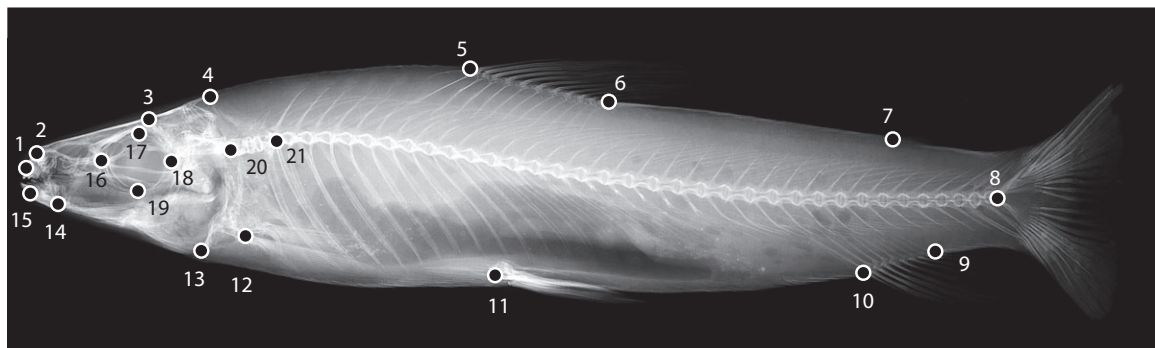

Figure 5. Radiograph of holotype of *Leporinus cylindriformis*, MCZ 20430, 188.0 mm standard length, showing position of 21 landmarks used in geometric morphometric analysis. Landmarks represent: (1) anterior limit of premaxilla; (2) dorsal tip of ascending process of premaxilla; (3) epiphyseal bar; (4) posterodorsal tip of supraoccipital; (5) origin of first dorsal-fin ray; (6) insertion of last dorsal-fin ray; (7) origin of adipose fin; (8) posterior extent of vertebral column and anterior of hypural plate, marked at midpoint of last vertebral centrum; (9) insertion of last anal-fin ray; (10) origin of first anal-fin ray; (11) pelvic-fin origin; (12) pectoral-fin origin; (13) ventral limit of joint between contralateral cleithra; (14) anguloarticular-quadrate joint; (15) anterior tip of dentary; (16) anterior limit of orbit; (17) dorsal limit of orbit; (18) posterior limit of orbit; (19) ventral limit of orbit; (20) joint between basioccipital and first vertebra of Weberian apparatus; (21) anterior limit of fifth vertebra (first vertebra not incorporated into Weberian apparatus and first bearing full sized pleural ribs). Image © President and Fellows of Harvard College.

ANOVA as implemented in PAST. Significant differences ($P \leq 0.05$) were determined with pairwise Tukey's post-hoc tests [a commonly used method to compare all pairs of subgroup means in an ANOVA framework (Whitlock & Schluter, 2009)]. Canonical variates analysis (Hotelling, 1935) was not employed because that method can overfit the separation amongst groups and produce unreliable results because of inadequate degrees of freedom when sample sizes are smaller than the number of measured variables (Weinberg & Darlington, 1976; Stevens, 2002), as they frequently are in museum-based studies of rare species.

GEOMETRIC MORPHOMETRICS

Twenty-one landmarks (Fig. 5) were located in tps-Dig2.1 (Rohlf, 2006) on digital radiographs of the specimens in lateral view. Most of these landmarks represent points that serve as endpoints in the set of linear measurements (Table 1), but several mark points of internal skeletal anatomy, such as the joint of the basioccipital with the first vertebra. Landmark configurations were subjected to Procrustes superimposition in MorphoJ v. 1.02b (Klingenberg, 2008), and an exploratory PCA was performed on the covariance matrix. As initial analyses revealed substantial ontogenetic shifts in morphology in all species for which juveniles were available, an allometric correction was necessary to compare the morphometrics of specimen series that differed in age and/or size structure. To that end, a pooled within-group allometric regression using log centroid size was performed on the Procrustes coordinates in MorphoJ. PCA using the covariance matrix of the residuals from the allometric regression (without further pooling by species) produced a size-standardized morphospace permitting meaningful comparisons of the morphology of specimens of different sizes. Note that because this protocol involved separating the predicted and residual components of variation and further interpreting the residuals, ordinary least squares regression and not RMA regression was preferred (Warton *et al.*, 2006). As the allometrically-corrected PCA yielded a morphospace with more than one important size-independent axis (see Results), subsequent analysis of amongst species-structure followed the MANOVA procedure in PAST. The sequential Bonferroni procedure was used to adjust significance levels for multiple post-hoc Hotelling's T^2 tests amongst all possible pairs of nominal species.

The holotype and paratype of *L. niceforoi* are both significantly bent, and although they could be physically straightened during calliper-based measurements, it proved impossible to generate nondistorted radiographs of these specimens. As a result, they were excluded from geometric morphometric analysis.

Table 1. Principal component (PC) loadings from traditional linear morphometrics

	PC1	PC2
Eigenvalue	1.362	0.018
Per cent variance explained	97.452	1.294
Snout to dorsal-fin origin	0.159	0.079
Snout to adipose-fin origin	0.164	0.138
Snout to anal-fin origin	0.166	0.138
Snout to pelvic-fin insertion	0.160	0.081
Snout to pectoral-fin insertion	0.144	−0.002
Dorsal origin to pectoral-fin insertion	0.173	−0.047
Dorsal origin to pelvic-fin insertion	0.171	**−0.307**
Dorsal origin to anal-fin origin	0.172	0.054
Dorsal origin to anal-fin insertion	0.169	0.138
Dorsal origin to hypural joint	0.166	0.170
Dorsal origin to adipose-fin origin	0.173	0.176
Length of dorsal-fin base	0.159	0.007
Dorsal-fin insertion to pelvic-fin origin	0.171	**−0.218**
Dorsal-fin insertion to adipose-fin origin	0.178	**0.266**
Dorsal-fin insertion to anal-fin origin	0.180	0.048
Dorsal-fin insertion to anal-fin insertion	0.174	0.162
Adipose-fin origin to anal-fin origin	0.167	**−0.238**
Adipose-fin origin to anal-fin insertion	0.169	−0.164
Adipose-fin origin to hypural joint	0.164	0.183
Length of anal-fin base	0.152	−0.005
Anal-fin insertion to hypural joint	0.152	0.139
Pelvic-fin insertion to anal-fin origin	0.176	0.192
Pelvic-fin insertion to adipose-fin origin	0.173	0.096
Pelvic-fin insertion to hypural joint	0.168	0.191
Pelvic-fin insertion to pectoral-fin insertion	0.177	**0.201**
Greatest body depth	0.171	**−0.308**
Greatest body width	0.184	−0.065
Caudal-peduncle depth	0.163	**−0.200**
Head length	0.145	−0.021
Preopercle length	0.147	−0.044
Snout to anterior margin of eye	0.165	−0.018
Head depth	0.161	**−0.352**
Snout depth	0.162	**−0.212**
Jaw length	0.161	−0.089
Eye diameter	0.123	−0.012
Interorbital width	0.167	**−0.217**
Snout to supraoccipital crest	0.143	0.018

The sign of all loadings on PC1 (which is highly correlated with standard length) have been reversed to facilitate allometric interpretation; the largest specimens have the highest, rather than the lowest scores on this axis after the reversal in sign.

On PC2, loadings with absolute magnitude greater than or equal to 0.2 appear in bold.

As the group membership of the types of *L. cylindriformis* and *L. niceforoi* was under investigation, we did not group those specimens with putative conspecifics during statistical tests. As a result, those specimens were excluded from some analyses because their implicit groups of $N = 1$ and $N = 2$ failed to meet minimum sample size requirements.

MERISTICS

Lateral line and transverse scale counts follow methods used in recent taxonomic studies of *Leporinus* (Britski & Garavello, 2005; Britski & Birindelli, 2008) with the addition of lower transverse scale counts reported at the anal-fin origin as well as at the pelvic-fin origin. The midline scale directly anterior to the first unbranched anal ray was not included in the lower transverse counts at the anal-fin origin. Other meristics follow Sidlauskas *et al*. (2007), with the only major difference between that study and those of Britski & Garavello (2005) and Britski & Birindelli (2008) being whether the last dorsal- and anal-fin rays, which are branched to the base, are counted as one or two rays. Following Fink & Weitzman (1974), Winterbottom (1980), Sidlauskas *et al*. (2007), and many other studies, these terminal divided rays are counted herein as a single element, a method of counting that reflects the underlying relationship of the rays to their pterygiophore.

RESULTS

LINEAR MORPHOMETRICS

PCA of the set of linear measurements summarized nearly 99% of the variation in these measures in two axes, with principal component one (PC1) and PC2 explaining 97.5 and 1.3% of total variance, respectively (Table 1). The remaining components explain negligible and nearly equivalent proportions of variance (e.g. 0.22, 0.16, and 0.13% on PC3, PC4, and PC5, respectively) and are indistinguishable from measurement error.

A scatterplot of PC1 versus PC2 shows considerable structure amongst *a priori* groups, although there is a complicated pattern of overlap (Fig. 6). Interpretation of amongst-group differences in this space is confounded by PC1's high correlation with standard length (Pearson product-moment correlation = 0.9932). If PC1 represented a pure scaling (size) isometric vector, the loadings of all variables on this axis would be 0.164 [calculated as $1/\sqrt{37}$ (Jolicoeur, 1963)], but the observed loadings rather range from 0.123 to 0.184, indicating that PC1 is instead an allometric vector describing correlated changes in shape and size. The measures with highest loading on PC1 include the width and depth of the body, whereas the measures with lowest loading include the diameter of the eye and the length of the head (Table 1). Taken as a whole, these PC1 loadings indicate that within each nominal species, as SL increases, the measures in the head region increase at a slower rate than do the postcranial measures. Juveniles have proportionally larger heads than do adults, a condition typical in fishes.

As PC1 represents allometric variation, raw separation amongst groups on this axis reflects differences in the size or age structure of the various samples and necessitates regression to test for amongst-group differences. Regressing the PC1 scores for the various species against SL (Fig. 7) reveals visually that the allometric trajectory describing proportionally larger heads and eyes in juveniles is universal for the examined species. Pair-wise tests for deviation from a common RMA slope reveal no amongst-species differences (Table 2, values below the diagonal). As a result of that shared slope, the variation in the *y*-intercept of the regression lines can be used as an additional test for amongst-group differences, and in fact there are interpretable differences in the *y*-intercepts of the regression lines amongst many pairs of species (Table 2, values above the diagonal). For example, the *y*-intercepts for *L. friderici* and *L. lebaili* are indistinguishable from each other but differ from all other species, reflecting the fact that these species have higher PC1 scores at any given standard length. In other words, the noticeably deeper bodies in *L. friderici* and *L. lebaili* are reflected by slightly longer raw linear measures. Similar, although more subtle variation is also revealed within the *L. cylindriformis* group proper (Table 2). *Leporinus apollo* in particular has a statistically lower intercept than all other examined species, and many other pairs of examined species are distinguishable on the basis of the PC1 intercept.

PC2 is not highly correlated with standard length (Pearson product-moment correlation = 0.1083), indicating that amongst-group differences on that axis are independent of specimen size and are interpretable directly as differences in shape. The measures with highest absolute loading on PC2 (Table 1) are primarily cross-body measures (dorsal-fin origin to pelvic-fin origin, head and body depth, adipose fin to anal-fin origin, etc.), indicating that PC2 indexes overall body depth, with the deepest-bodied species (*L. lebaili*, *L. friderici*) located at the negative extreme and the most slender species (*L. apollo, L. cylindriformis, L. niceforoi*) at the positive extreme (Fig. 6).

ANOVA on the PC2 scores reveals amongst-group structure similar but not identical to that returned by the intercept-based tests on PC1 (Table 3). In general, species at one extreme of variation (e.g. *L.*
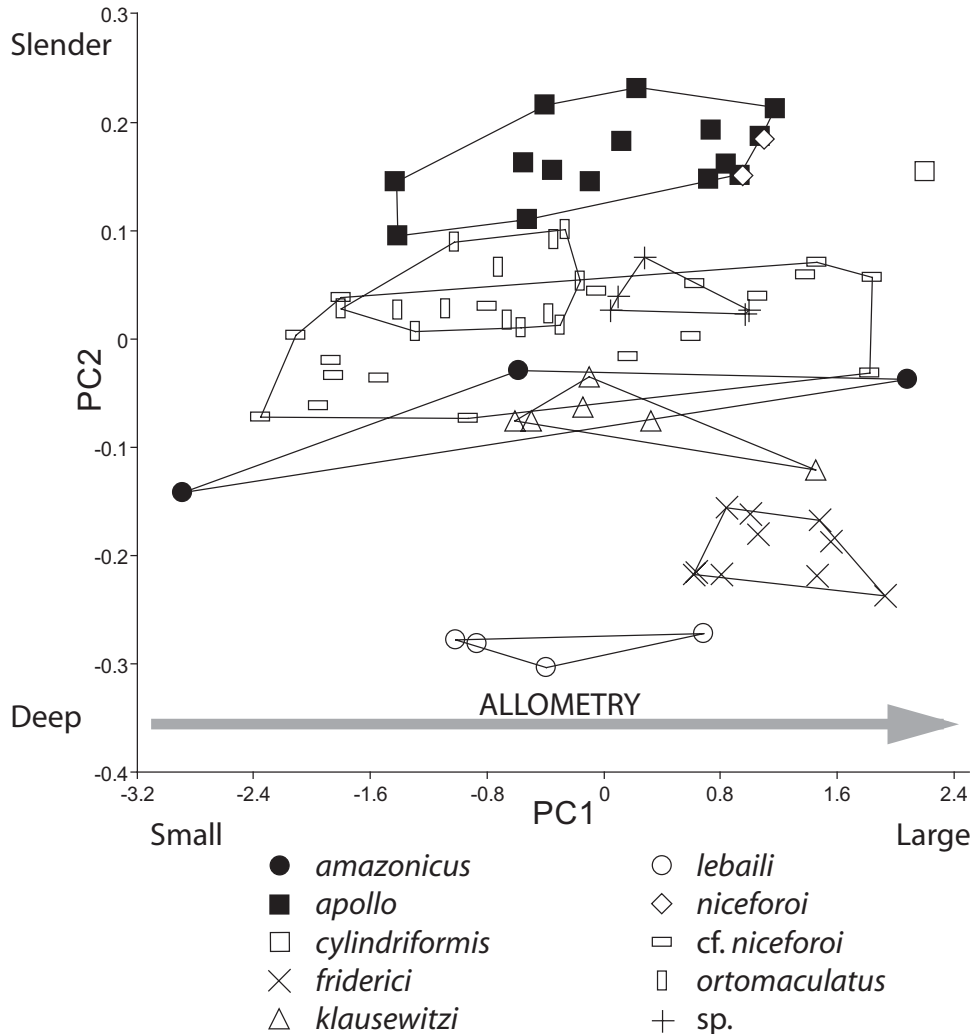
Figure 6. Scatterplot of principal component two (PC2) versus one from traditional linear morphometrics for species of *Leporinus* discussed in text. PC1 is an allometric vector describing size and shape variation, whereas PC2 is essentially size-free. Polygons indicate convex hulls.

apollo) can easily be distinguished from those at the opposite extreme, whereas more intermediate species are indistinguishable based on PC2 alone. For example *L. ortomaculatus*, *L.* cf. *niceforoi*, and *Leporinus*. sp. cluster closely, have largely overlapping PC2 scores, and cannot be reliably separated on PC2 (Table 3).

The holotype and paratype of *L. niceforoi*, which originated in Colombia, proved statistically separable from the putatively conspecific specimens from Ecuador and Peru on the basis of slightly lesser body depth (Table 3). Although it could not be included in statistical tests, the holotype of *L. cylindriformis* also falls outside the range of its putative conspecifics (*Leporinus* sp.) on PC2 (Fig. 6). The only examined specimens as slender as the types of *L. cylindriformis*

and *L. niceforoi* were the series of recently collected specimens from Suriname described herein as *L. apollo*.

GEOMETRIC MORPHOMETRICS

Prior to allometric correction, PCA of the landmark configurations taken from radiographs yielded results that were generally similar to those from the analysis of linear measurements. Three components summarized in total 80.4% of the variance in the landmark coordinates following Procrustes superimposition, with PC1, PC2, and PC3 summarizing 48.6, 16.9, and 14.9% of that variance, respectively. The remaining components each indexed 4.7% or less of total variance.
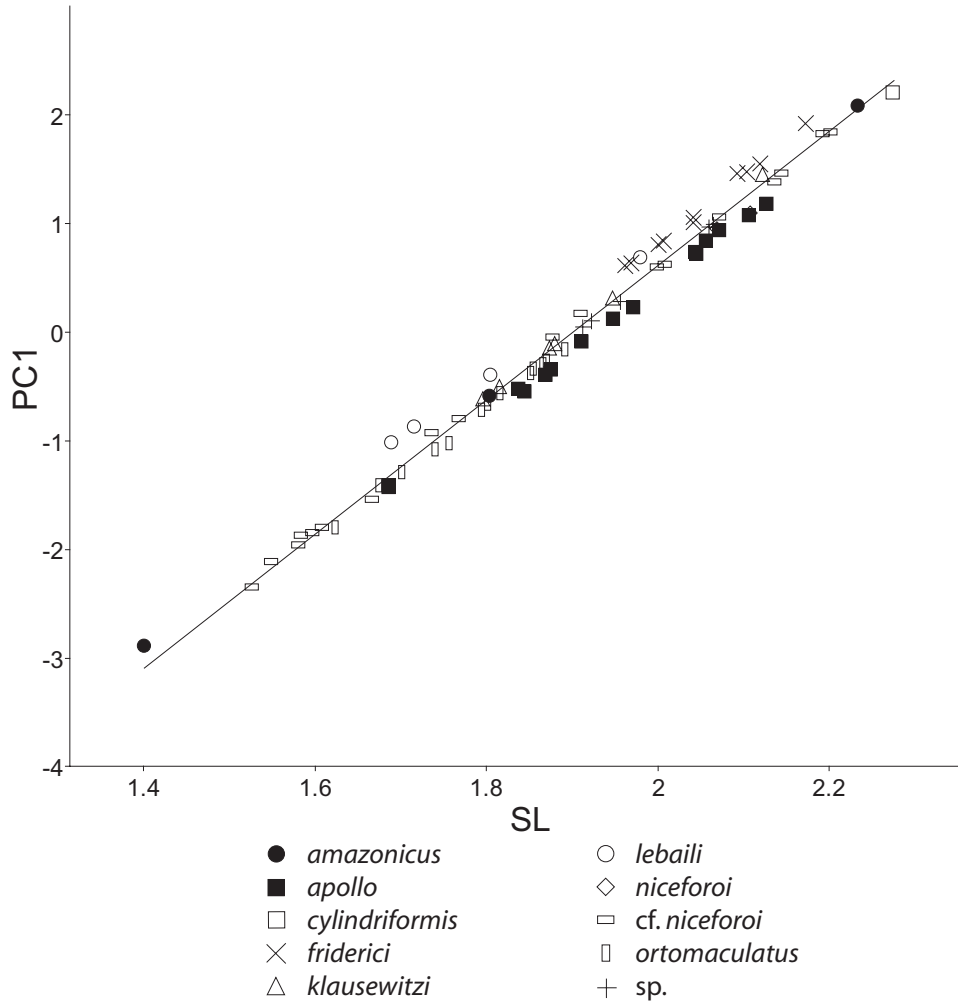
Figure 7. Reduced major axis regression of principal component one (PC1) scores from traditional linear morphometrics on log standard length for species of *Leporinus* discussed in text. Trendline represents a universal regression that does not take species membership into account; tests for equivalence of slope and intercept as reported in Tables 2 and 3 estimate a separate regression line for each putative species.

Despite the removal of variation because of scaling, translation, and rotation during the Procrustes fit, all three of the most important components correlate at least moderately with log centroid size (Pearson product-moment correlations of −0.340, −0.756 and 0.318, for PC1–3, respectively). Those values indicate that the allometric shape change is distributed across multiple axes rather than being confined to a single axis as it was in the analysis of linear measurements. This effect is apparent in a scatterplot of PC2 versus PC1 (Fig. 8), which resembles a rotated and reflected version of the similar scatter from the linear analysis (Fig. 6). Both figures reveal similar patterns of overlap and non-overlap amongst groups, but in the two-dimensional visualization from geometric morphometrics (Fig. 8) the line of allometry runs obliquely from upper right to lower left and is not aligned with PC1 as it was in the analysis of linear measurements (Fig. 6).

As a result of the strong allometric signal in the geometric data, effective analysis of amongst-group structure required separating the scale-dependent and scale-independent aspects of variation through least-squares regression of the Procrustes coordinates on log centroid size. The scale-dependent (allometric) shape variation described by the regression line primarily indexes variation in the relative size of the head and eye, as visualized by the wireframe diagram in Figure 9. This variation matches precisely the variation described by the allometric PC1 from the linear analysis (Table 1).

Table 2. *P*-values from pairwise analyses in SMATR of reduced major axis regressions of principal component one (PC1) scores on log-transformed standard length

	Leporinus amazonicus	*Leporinus apollo*	*Leporinus friderici*	*Leporinus klausewitzi*	*Leporinus lebaili*	*Leporinus* cf. *niceforoi*	*Leporinus ortomaculatus*	*Leporinus* sp.
L. amazonicus		**0.0000**	0.0184	0.6761	**0.0049**	0.2890	**0.0051**	0.1642
L. apollo	0.7240		**0.0000**	**0.0000**	**0.0000**	**0.0000**	**0.0000**	**0.0000**
L. friderici	0.1127	0.1145		**0.0000**	0.6796	**0.0000**	**0.0000**	**0.0000**
L. klausewitzi	0.3342	0.0051	0.7677		**0.0000**	0.1159	**0.0000**	**0.0000**
L. lebaili	0.6682	0.3588	0.0523	0.1006		**0.0000**	**0.0000**	**0.0000**
L. cf. *niceforoi*	0.5147	0.4517	0.1930	0.0160	0.2385		**0.0000**	0.0614
L. ortomaculatus	0.4538	0.5356	0.2486	0.1134	0.2210	0.9311		0.0656
L. sp.	0.2443	0.1806	0.7157	0.8560	0.1199	0.2969	0.3650	

Values below the diagonal represent likelihood ratio tests for differences in slope, values above the diagonal represent tests for differences in intercept. Bold numbers represent statistically significant *P*-values following sequential Bonferroni correction at a table-wide alpha level of 0.05, with slope and elevation tests treated as separate tables for the purpose of the Bonferroni correction.

The holotype of *Leporinus cylindriformis* and the holotype and paratype of *Leporinus niceforoi* were excluded because the statistical tests require that the regression lines be determined by a minimum of three points.

Table 3. *Q*-values (below diagonal) and *P*-values (above diagonal) for post-hoc Tukey's pairwise comparisons from analysis of variance on principal component two (PC2) scores from linear morphometrics

	Leporinus amazonicus	*Leporinus apollo*	*Leporinus friderici*	*Leporinus klausewitzi*	*Leporinus lebaili*	*Leporinus niceforoi* (types)	*Leporinus* cf. *niceforoi*	*Leporinus ortomaculatus*	*Leporinus* sp.
L. amazonicus		**0.0001**	**0.0009**	0.9132	**0.0001**	**0.0001**	0.2206	**0.0050**	**0.0083**
L. apollo	11.90		**0.0001**	**0.0001**	**0.0001**	1.0000	**0.0001**	**0.0012**	**0.0007**
L. friderici	6.38	18.28		0.0556	0.0616	**0.0001**	**0.0001**	**0.0001**	**0.0001**
L. klausewitzi	1.90	13.80	4.47		**0.0001**	**0.0001**	**0.0063**	**0.0002**	**0.0002**
L. lebaili	10.80	22.70	4.42	8.89		**0.0001**	**0.0001**	**0.0001**	**0.0001**
L. niceforoi (types)	11.94	0.04	18.32	13.85	22.74		**0.0001**	**0.0011**	**0.0007**
L. cf. *niceforoi*	3.63	8.27	10.01	5.53	14.43	8.31		0.8850	0.9387
L. ortomaculatus	5.64	6.26	12.02	7.55	16.44	6.30	2.01		1.0000
L. sp.	5.41	6.49	11.79	7.32	16.21	6.53	1.79	0.23	

Bold numbers represent statistically significant *P*-values at an alpha level of 0.05. The holotype of *L. cylindriformis* was excluded because the tests require at least two individuals in each sample.
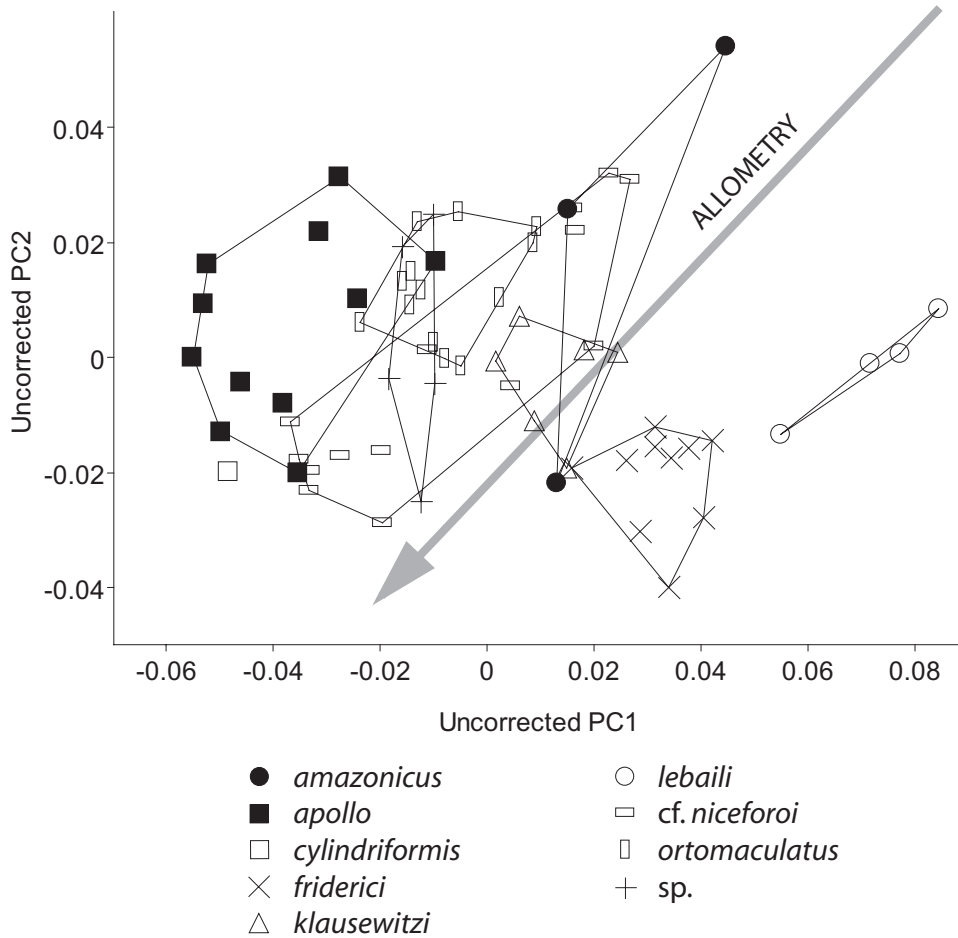
Figure 8. Scatterplot of principal components one and two from geometric morphometric analysis without allometric correction for species of *Leporinus* discussed in text. Both axes show significant correlations with log centroid size.

Figure 9. Wireframe visualization of allometric shape change along the least squares regression line of Procrustes coordinates on log centroid size. Grey landmarks represent the average configuration amongst all specimens, whereas black landmarks represent the approximate extreme of variation (1.2 log centroid size units) in the direction of the smallest specimens, which have proportionally larger heads and eyes.

PCA of the residuals from the allometric regression returned a dataset with three important axes. 53.3% of the scale-independent variance was summarized on PC1, 18.4% on PC2, and 6.2% on PC3 for a total of 78.0%. The wireframes in Figure 10 visualize the shape change on each of these axes. PC1 clearly

describes the overall depth of the body and is similar in interpretation to PC2 from the analysis of linear measurements. The geometric PC2 describes subtle variation in the position of the mouth and curvature in the profile of the body, with positively scoring specimens having slightly more subterminal mouths, higher dorsal-fin bases, and more ventrally positioned caudal peduncles. PC3 describes variation in the anteroposterior elongation of the head and the dorsoventral tapering of the posterior half of the body. Although the variation indexed by PC3 is subtle, it is biologically interpretable and exhibits clear structure amongst putative species (see below). The remaining axes each summarize 5.1% or less of total variance.

A scatterplot of the allometrically corrected axes from geometric analysis reveals clear separation of nominal species along PC1 and PC3 (Fig. 11). PC1 segregates species by average body depth. *Leporinus lebaili* has the most positive score on this axis and the deepest body morphology, with *L. friderici* a close second. *Leporinus amazonicus* and *L. klausewitzi*
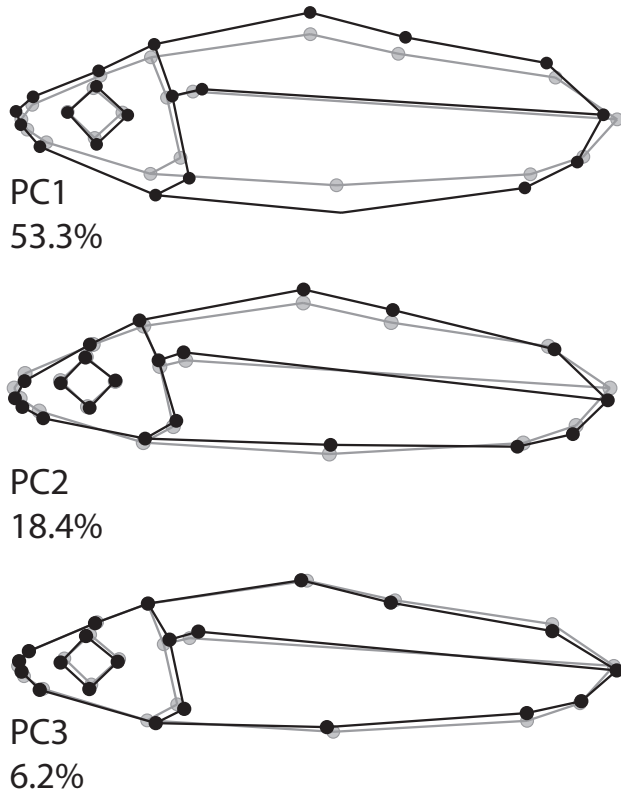
Figure 10. Wireframe visualization of variation along the allometrically corrected principal components one (PC1), two, and three from geometric morphometric analysis. Grey landmarks represent the configuration of the average specimen, black landmarks represent one approximate extreme of variation on that axis. The deformation on PC1 represents 0.07 units, that on PC2 represents 0.04 units, and that on PC3 represents 0.03 units. Percentages indicate the proportion of total variance amongst the Procrustes residuals explained by each axis.

have overlapping and intermediate morphologies. *Leporinus ortomaculatus*, *L.* cf. *niceforoi*, and *Leporinus* sp. form a fourth closely overlapping group that is more dorsoventrally slender than are the previous four species. Finally, *L. apollo* occupies the slender extreme of observed variation on PC1, with the *L. cylindriformis* holotype falling near the least slender examples of *L. apollo* and the most slender examples of *L. ortomaculatus*.

Despite its relatively small percentage of overall variation, PC3's information on head length and the degree of tapering of the posterior half of the body provides information that is critical to the separation of several nominal species (Fig. 11B). Notably, PC3 completely segregates *L. apollo* from *L. cylindriformis*, *L. amazonicus* from *L. klausewitzi*, and *L. ortomaculatus* from *L.* cf. *niceforoi* and *Leporinus* sp., despite the similarity of these species on PC1. When

PC1 and PC3 are considered simultaneously in a scatterplot (Fig. 11B), only the convex hulls for *L.* cf. *niceforoi* and *Leporinus* sp. overlap substantially. MANOVA on the set of all three geometric axes confirms the statistical separation of all species pairs except this last (Table 4, values above the diagonal). When PC3 is excluded (Table 4, values below the diagonal), four comparisons amongst species lose significance.

Contrasting with the PC1 and PC3 results, very little separation amongst species exists on PC2. The curvature in body form described by that axis (Fig. 10) might be a general biological characteristic of *Leporinus*, or could reflect an artefact of preservation or parallax related to the random offset of specimens under the point source of X-rays rather than biological variation.

Meristics

Variation in the number of vertebrae and transverse scales is useful in further distinguishing species in the *L. cylindriformis* complex (Table 5). In particular, the upper transverse scale count serves to distinguish *L. cylindriformis* and *L. apollo* (typically with six scales in this series) from all other examined species (five scales in this series except for six in one specimen of *L.* cf. *niceforoi*). The 38 or 39 vertebrae possessed by *L. cylindriformis* and *L. apollo* further distinguish those species from *L. amazonicus* (which invariably has 41 vertebrae) and from *L. friderici*, *L. ortomaculatus*, *L. lebaili*, and *L. klausewitzi*, all of which consistently have 37 or fewer vertebrae. *Leporinus* sp., *L. niceforoi*, and *L.* cf. *niceforoi* all contain individuals with 38 or 39 vertebrae. The species in the *L. cylindriformis* group also assort partially in lateral-line scale counts, but there is significant overlap in the range of this count amongst species (Table 5). The remaining examined meristics are not diagnostic with respect to species membership.

DISCUSSION

ALLOMETRY AND MAJOR AXES OF SHAPE VARIATION

Analyses of linear measurements and of landmark coordinates confirmed independently that allometry contributes importantly to shape variation within the examined species of *Leporinus*. The combined effects of scale and allometry summarized on PC1 dominated the linear measurements, including over 97% of total variation (Table 1, Figs 6, 7). In the geometric dataset, even with removal of isometric scaling via the Procrustes fit, scale-correlated shape change contributed to the most important remaining axes of variation (Fig. 8). Tests for changes in the slope of the allometric trajectory amongst all pairs of species
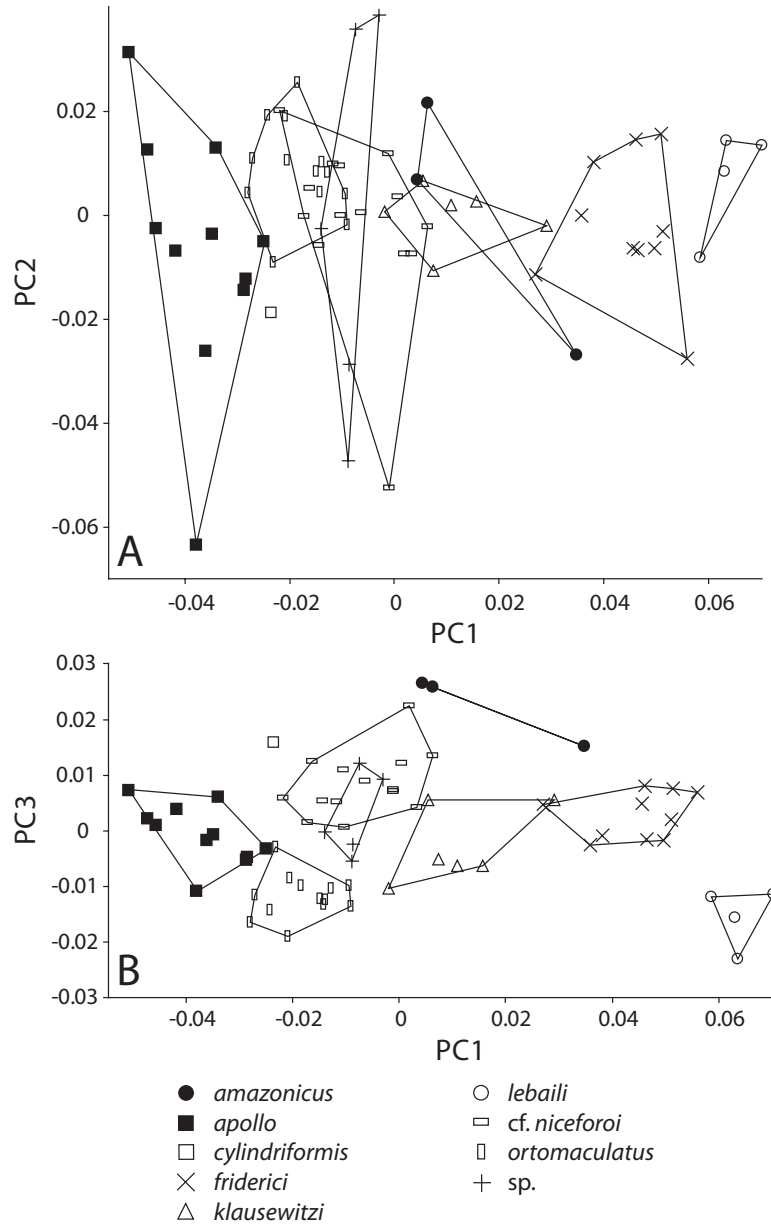
Figure 11. Scatterplot of (A) principal components one and two and (B) principal components one and three from geometric morphometrics after allometric correction. Polygons represent convex hulls surrounding nominal species of *Leporinus*.

revealed that examined species all share the basic nature of the allometry (Table 2, Fig. 7). Visualization of the allometric trajectory after it had been regressed out of the geometric dataset indicated that the size of the head and eye becomes proportionally smaller as juveniles grow into adults (Fig. 9). As the effects of within-species allometry were so strong in this dataset, regression-based corrections for those effects were required to reveal size-independent shape differences amongst the *a priori* groupings of specimens.

Once allometric effects were accounted for, the single most important remaining axis of variation was body depth. PC2 from the linear analysis and PC1 from the allometrically corrected geometric dataset indexed that variation most completely. Analysing the intercepts of the regression of the linear PC1 against standard length also recovered variation in slenderness amongst species, with the slenderest species possessing the lowest Y-intercepts. PC3 from the corrected geometric dataset revealed additional

Table 4. *P*-values for pairwise Hotelling's comparisons from multivariate analysis of variance on scores for first two principal component (PC) axes (below diagonal) or first three PC axes (above diagonal) from geometric morphometrics

	Leporinus amazonicus	*Leporinus apollo*	*Leporinus friderici*	*Leporinus klausewitzi*	*Leporinus lebaili*	*Leporinus cf. niceforoi*	*Leporinus ortomaculatus*	*Leporinus sp.*
L. amazonicus		**0.0000**	**0.0006**	**0.0126**	**0.0160**	**0.0031**	**0.0000**	**0.0001**
L. apollo	**0.0000**		**0.0000**	**0.0000**	**0.0000**	**0.0000**	**0.0000**	**0.0000**
L. friderici	**0.0042**	**0.0000**		**0.0001**	**0.0001**	**0.0000**	**0.0000**	**0.0000**
L. klausewitzi	0.8384	**0.0000**	**0.0001**		**0.0002**	**0.0000**	**0.0000**	**0.0062**
L. lebaili	**0.0054**	**0.0000**	**0.0060**	**0.0002**		**0.0000**	**0.0000**	**0.0000**
L. cf. niceforoi	**0.0042**	**0.0000**	**0.0000**	**0.0025**	**0.0000**		**0.0042**	0.2772
L. ortomaculatus	**0.0001**	**0.0000**	**0.0000**	**0.0000**	**0.0000**	**0.0000**		**0.0001**
L. sp.	0.0808	**0.0000**	**0.0000**	0.0190	**0.0000**	0.9502	0.0176	

Bold numbers represent statistically significant *P*-values following sequential Bonferroni correction at a table-wide alpha level of 0.05. The holotype of *Leporinus cylindriformis* was excluded because the tests require at least two individuals in each sample, and the holotype and paratype of *Leporinus niceforoi* were excluded because they are significantly bent and could not be imaged without distortion.

aspects of variation that were uncorrelated with the size of the specimens, namely the anteroposterior length of the head and the degree of dorsoventral tapering of the posterior half of the body. This subtle variation on the geometric PC3 proved crucial in distinguishing amongst several pairs of species, and would not have been apparent without allometric correction.

THE ABILITY OF ALLOMETRIC CORRECTION TO IMPROVE DISCRIMINATION AMONGST GROUPS

Both the linear dataset and the geometric dataset effectively separated many of the *a priori* groups, but such separation was achieved only after allometry was properly considered via regression. In the geometric dataset, simple PCA following Procrustes superimposition produced a morphospace in which nearly every species was broadly overlapping (Fig. 8) and not statistically distinguishable. Regressing out the component of variation due to allometry (Fig. 9) visually (Fig. 11) and statistically (Table 4) separated all but a single pair of nominal species, greatly improving the power of the analysis. This point is well worth emphasizing, because it highlights that the Procrustes fit used in geometric analysis does not remove the confounding effects of size on shape from the dataset. Only by correcting for shape difference amongst groups resulting from differences in the size of the available specimens can one test for consistent shape differences amongst groups.

In the linear dataset, because size and shape variation both contributed to variation along the most important component of variation in the linear dataset (PC1), differences in the size structure of the samples resulted in spurious separation amongst groups on PC1 (Fig. 6). This over-separation of groups presents a slightly different but potentially more insidious problem than was observed in the geometric case (in which groups were overlapping prior to allometric correction), because it could lead to over-splitting of species if not recognized. A simple and common correction for this problem would discard the size-correlated PC1 and analyse only the shape variation orthogonal to that axis (PC2 in this dataset). Analysing only PC2 (Table 3) would have failed to distinguish several pairs of species that were highly separable using the characteristic intercept of the PC1 regression for each group (Table 2), including *L. ortomaculatus*/*L.* cf. *niceforoi* and *L. friderici*/*L. klausewitzi* (see also Fig. 7). Even when an additional correction to the higher numbered PCs is applied through sheared PCA (Humphries *et al.*, 1981) or Burnaby's (1966) method, a significant proportion of shape variation can be lost through the exclusion of PC1 if allometry is strong (Bookstein *et al.*, 1985). If

Table 5. Meristic counts summarized as ranges followed by the mean ± 1 standard deviation in parentheses. Single values in a cell indicate invariable counts amongst the examined specimens for a given species

	Leporinus amazonicus	*Leporinus apollo*	*Leporinus cylindriformis*	*Leporinus friderici*	*Leporinus klausewitzi*
Unbranched dorsal-fin rays	ii	ii	ii	ii	ii
Branched dorsal-fin rays	10	10	10	10	10
Unbranched anal-fin rays	iii	iii	iii	iii	iii
Branched anal-fin rays	8	7–8* (7.9 ± 0.3)	8	8	8
Unbranched pectoral-fin rays	i	i	i	i	i
Branched pectoral-fin rays	14–15 (14.5 ± 0.7)	14–16; 15* (15.1 ± 0.6)	16	15–16 (15.2 ± 0.4)	14–16 (15.2 ± 1.0)
Unbranched pelvic-fin rays	i	i	i	i	i
Branched pelvic-fin rays	8	8	8	7–9 (7.9 ± 0.6)	8
Upper principal caudal-fin rays	10	10	10	10	10
Lower principal caudal-fin rays	9	9	9	9	9
Lateral line scales to anterior margin of hypural plate	38–40 (38.7 ± 1.2)	35†–39; 37* (36.8 ± 1.0)	37	32–34 (33.3 ± 0.7)	34–35 (34.5 ± 0.5)
Scales over hypural plate	5–6 (5.3 ± 0.6)	4†–5* (4.9 ± 0.4)	5	4–5 (4.4 ± 0.5)	3–5 (4.3 ± 0.8)
Total lateral line scales	43–45 (44.0 ± 1)	40†–44; 42* (41.7 ± 1.1)	42	37–39 (37.7 ± 0.7)	38–40 (36.8 ± 0.8)
Upper transverse scales at dorsal-fin origin	5	5–6* (5.9 ± 0.3)	6	5	5
Lower transverse scales at pelvic-fin origin	4.5–5 (4.8 ± 0.3)	4–5* (4.8 ± 0.4)	5	4–5 (4.9 ± 0.3)	4–5 (4.8 ± 0.4)
Lower transverse scales at anal-fin origin	4	4	4	4	4
Circumpeduncular scales	16	16	16	16	16
Predorsal scales	12–14 (13.0 ± 1.4)	11–15; 14* (13.2 ± 1.5)	11	11–12 (11.1 ± 0.3)	10–12 (11.3 ± 0.8)
Premaxillary teeth	4	3–4* (3.9 ± 0.3)	4	4	4
Dentary teeth	4	3–4* (3.8 ± 0.4)	4	4	4
Vertebrae	41	38*–39 (38.3 ± 0.5)	36–39 (37.8 ± 1.1)	34–35 (34.8 ± 0.4)	36–37 (36.8 ± 0.4)

	L. lebaili	*L. niceforoi*	*L.* cf. *niceforoi*	*L. ortomaculatus*	*L.* sp.
Unbranched dorsal-fin rays	ii	ii	ii	ii	ii
Branched dorsal-fin rays	10	10	10	10	10
Unbranched anal-fin rays	iii	iii	iii	iii	iii
Branched anal-fin rays	8	8	8	8	8
Unbranched pectoral-fin rays	i	i	i	i	i
Branched pectoral-fin rays	15–16 (15.5 ± 0.6)	16.5	14–16 (15.1 ± 0.7)	15–17 (15.8 ± 0.6)	16–17 (16.6 ± 0.5)
Unbranched pelvic-fin rays	i	i	I	i	I
Branched pelvic-fin rays	8	8	8	8	8–9 (8.2 ± 0.4)
Upper principal caudal-fin rays	9–10 (9.8 ± 0.5)	Missing	10	10	10
Lower principal caudal-fin rays	9	Missing	9	9	9
Lateral line scales to anterior margin of hypural plate	31–33 (32.0 ± 0.8)	35–36 (35.5 ± 0.7)	34–38 (36.3 ± 1.2)	33–36 (34.5 ± 1.0)	35–36 (35.6 ± 0.5)
Scales over hypural plate	3–5 (4.3 ± 1.0)	5–6 (5.5 ± 0.7)	4–6 (4.6 ± 0.7)	3–5 (4.4 ± 0.7)	4–5 (4.8 ± 0.4)
Total lateral line scales	36–37 (36.3 ± 0.5)	41	38–43 (40.9 ± 1.5)	38–41 (38.9 ± 1.0)	40–41 (40.4 ± 0.5)
Upper transverse scales at dorsal-fin origin	5	5	4–6 (5.0 ± 0.3)	5	5
Lower transverse scales at pelvic-fin origin	5	4	4–5 (4.2 ± 0.4)	4–5 (4.2 ± 0.3)	4–5 (4.5 ± 0.5)
Lower transverse scales at anal-fin origin	4–5 (4.5 ± 0.6)	4	4–5 (4.1 ± 0.2)	4	4
Circumpeduncular scales	16	16	16	16	16
Predorsal scales	10–12 (10.8 ± 1.0)	11–14 (12.5 ± 2.1)	11–14 (12.0 ± 0.9)	11–12 (11.4 ± 0.5)	11–12 (11.6 ± 0.5)
Premaxillary teeth	4	4	4	4	4
Dentary teeth	4	4	3–4 (3.9 ± 0.4)	4	4
Vertebrae	35–36 (35.5 ± 0.6)	39	36–39 (37.8 ± 1.1)	36	38

*Values of varying counts for the *L. apollo* holotype.
†Values exclude a specimen with a malformed hypural plate and only 38 total lateral-line scales.

this dataset is at all typical, our analysis implies that to maximize the discriminatory power of a morphometric dataset, variation on PC1 should be analysed explicitly using regression rather than discarded.

Based on the clear improvement to both analyses provided by the allometric correction, we conclude that such a correction should be more frequently used in taxonomic studies that rely heavily upon morphometrics. The routines for performing these analyses in SMATR and especially MorphoJ are easily implemented and freely available, and there should be no logistical barrier to their wider adoption. At best, failure to use these or other allometric alternatives will prevent such studies from realising the full potential of their data, and at worst, may cause the resulting diagnoses to be built upon spurious shape differences that are not consistent across ontogeny.

COMPARISON BETWEEN LINEAR AND GEOMETRIC APPROACHES

The patterns of separation returned by the two types of analyses were largely congruent, with all of the species pairs that were separated by linear morphometrics also segregated by geometric morphometrics. However, the geometric analysis was able to separate four more species pairs than did the linear analysis: *L. amazonicus* from *L. klausewitzi*, L. cf. *niceforoi* and *Leporinus* sp., and *L. friderici* from *L. lebaili*. At least in this instance, the geometric methods appear to have more power than do traditional linear methods. Fink & Zelditch (1997), Parsons *et al.* (2003), and Maderbacher *et al.* (2008) reached similar conclusions, and if these collective results indicate a general trend, then the geometric methods for species discrimination should be preferred over their linear analogues whenever possible. That said, the discriminatory ability of the linear approach is still excellent, provided that it includes explicit analysis of allometric vectors (PC1 in this and many other case studies). Our recommendation in favour of the geometric approach should not be interpreted as a condemnation of the traditional linear method!

Despite the higher power of the geometric approach, the traditional approach has two advantages. First, it permits the inclusion of bent specimens like the type series of *L. niceforoi*, provided one can straighten them sufficiently to permit accurate calliper measurements. Such specimens cannot be imaged without significant distortion or foreshortening, and cannot be used in geometric analyses. Second, the traditional approach permitted the inclusion of measurements of width (body width and infraorbital width in this example) not obtainable from the radiographs from which the 2D landmark data were taken. Although geometric techniques exist for collecting and analysing 3D data, such protocols require expensive and unusual equipment such as 3D scanners or microscribes. When such equipment is unavailable and 3D structure is suspected to contain important signal, linear measurements present a workable alternative.

The meristic dataset proved insufficient to distinguish amongst most pairs of specimens, but provided important supplementary information that helped to separate certain species pairs. *Leporinus amazonicus*, for example, was indistinguishable from *L. klausewitzi* on the basis on linear morphometrics (Tables 2, 3), but the two species are easily separated on the basics of lateral-line scale and vertebral counts (Table 5).

A NEW SPECIES FROM SURINAME

The elongate specimens from Suriname that originally sparked this study (*L. apollo*) are widely separated in morphometrics from all species in the *L. cylindriformis* group except for the holotype of *L. cylindriformis*, the holotype and paratype of *L. niceforoi*, and some specimens of *L. ortomaculatus* (Figs 6, 11). *Leporinus ortomaculatus* and the *L. niceforoi* types are separable from *L. apollo* on the basis of meristics (Table 5) and coloration (see formal diagnosis below). This leaves only *L. cylindriformis* as a potential match. *Leporinus apollo* is very similar to the *L. cylindriformis* holotype; the two groups are identical in meristic counts (Table 5), and indistinguishable via the linear morphometric PC2 (Fig. 6). However, they are separated via geometric morphometrics (Fig. 11), where the *L. cylindriformis* holotype falls outside the convex hull and 95% confidence ellipse (not shown graphically) surrounding *L. apollo*. Body width, which does not load highly on the traditional PC2 (Table 1), provides a further linear diagnosis. In the *L. cylindriformis* holotype the percentage of the width of the body in SL (15.2%) falls outside the range of variation (9.7–14.0%) and more than two standard deviations from the mean (11.9%) of *L. apollo* (Table 6). Although slight, the variation in the width of the body represents a diagnosable linear difference, which combined with notable differences in coloration (see diagnosis below) and the clear geometric distinction (Fig. 11), reliably separates *L. apollo* from *L. cylindriformis*. Based on those differences, we describe the new species formally below.

LEPORINUS APOLLO SP. NOV.

Leporinus cf. *cylindriformis*, Willink & Sidlauskas 2006: 106 (photograph, partial morphometrics and meristics of specimen designated herein as holotype, suggestion of undescribed status).

Table 6. Traditional linear morphometrics for all examined species summarized as observed ranges, with mean ± standard deviation, in parentheses. Standard length (SL) appears in millimetres. Measures 1 to 29 are percentages of SL, measures 30 to 37 are percentages of head length

		Leporinus apollo (holotype)	*L. eporinus apollo*	*Leporinus cylindriformis* (holotype)
	Standard length	111.1	48.6–133.9 (90.9 ± 27.3)	188.0
1	Snout to dorsal-fin origin	48.5	45.4–48.5 (47.4 ± 1.0)	47.4
2	Snout to adipose-fin origin	86.8	83.7–88.6 (86.5 ± 1.3)	89.1
3	Snout to anal-fin origin	81.6	79.8–84.3 (82.3 ± 1.3)	85.4
4	Snout to pelvic-fin insertion	50.9	47.0–53.1 (50.7 ± 1.4)	49.2
5	Snout to pectoral-fin insertion	25.2	23.8–29.6 (26.5 ± 1.7)	24.4
6	Dorsal origin to pectoral-fin insertion	27.9	25.3–28.9 (26.8 ± 1.0)	28.2
7	Dorsal origin to pelvic-fin insertion	22.4	18.5–22.4 (20.6 ± 1.2)	21.5
8	Dorsal origin to anal-fin origin	40.6	38.8–42.3 (40.7 ± 1.0)	43.8
9	Dorsal origin to anal-fin insertion	49.0	45.7–59.9 (48.3 ± 1.5)	50.8
10	Dorsal origin to hypural joint	54.2	51.4–56.6 (54.6 ± 1.6)	56.3
11	Dorsal origin to adipose-fin origin	41.3	38.0–43.4 (41.0 ± 1.8)	43.4
12	Length of dorsal-fin base	13.6	12.8–14.9 (13.9 ± 0.7)	14.4
13	Dorsal-fin insertion to pelvic-fin origin	21.5	18.2–23.0 (20.5 ± 1.4)	20.4
14	Dorsal-fin insertion to adipose-fin origin	26.7	24.1–29.1 (27.2 ± 1.7)	29.2
15	Dorsal-fin insertion to anal-fin origin	28.6	24.7–30.0 (27.4 ± 1.4)	30.2
16	Dorsal-fin insertion to anal-fin insertion	34.6	31.6–35.8 (34.2 ± 1.2)	36.4
17	Adipose-fin origin to anal-fin origin	14.0	12.0–14.5 (13.6 ± 0.7)	14.0
18	Adipose-fin origin to anal-fin insertion	10.8	9.5–12.1 (10.9 ± 0.8)	11.8
19	Adipose-fin origin to hypural joint	14.3	12.4–15.4 (14.2 ± 0.8)	14.3
20	Length of anal-fin base	8.5	7.6–10.2 (9.0 ± 0.8)	9.0
21	Anal-fin insertion to hypural joint	9.3	9.0–11.6 (9.6 ± 0.7)	9.5
22	Pelvic-fin insertion to anal-fin origin	31.4	30.1–33.6 (32.1 ± 1.1)	35.9
23	Pelvic-fin insertion to adipose-fin origin	39.2	37.5–43.0 (39.7 ± 1.3)	42.7
24	Pelvic-fin insertion to hypural joint	50.3	48.8–52.4 (50.8 ± 1.1)	51.9
25	Pelvic-fin insertion to pectoral-fin insertion	26.7	23.5–28.6 (25.6 ± 1.3)	25.4
26	Greatest body depth	21.8	18.3–22.9 (20.7 ± 1.3)	21.5
27	Greatest body width	12.2	9.7–14.0 (11.9 ± 1.1)	15.2
28	Caudal-peduncle depth	8.0	7.4–9.3 (8.3 ± 0.6)	8.7
29	Head length	23.3	23.1–26.3 (24.6 ± 1.1)	23.5
30	Preopercle length	80.4	74.0–80.4 (77.2 ± 2.1)	78.0
31	Snout to anterior margin of eye	41.7	34.5–42.4 (38.9 ± 2.4)	44.6
32	Head depth	72.3	62.7–72.3 (68.1 ± 2.8)	71.5
33	Snout depth	43.5	39.7–45.3 (42.9 ± 1.4)	46.5
34	Jaw length	22.5	17.1–23.9 (20.8 ± 2.0)	24.8
35	Eye diameter	27.5	25.4–32.0 (28.1 ± 1.7)	24.9
36	Interorbital width	33.4	30.8–38.0 (33.8 ± 1.9)	35.3
37	Snout to supraoccipital crest	94.2	87.2–97.3 (93.6 ± 2.5)	93.7

		Leporinus amazonicus	*Leporinus friderici*	*Leporinus klausewitzi*
	Standard length	25.2–170.7 (64.9 ± 75.4)	91.5–148.3 (113.5 ± 18.5)	62.4–132.3 (83.1 ± 25.8)
1	Snout to dorsal-fin origin	46.4–51.6 (48.7 ± 2.6)	48.0–51.8 (49.6 ± 1.2)	48.6–50.1 (49.4 ± 0.6)
2	Snout to adipose-fin origin	85.5–87.5 (86.5 ± 1.0)	87.8–90.3 (88.6 ± 0.9)	85.6–87.5 (86.8 ± 0.8)
3	Snout to anal-fin origin	78.9–83.1 (80.7 ± 2.1)	83.4–87.1 (84.7 ± 1.2)	79.0–81.9 (80.8 ± 1.2)
4	Snout to pelvic-fin insertion	51.3–54.6 (52.6 ± 1.7)	52.3–56.1 (53.8 ± 1.1)	50.3–52.3 (51.2 ± 0.8)
5	Snout to pectoral-fin insertion	28.9–35.7 (32.0 ± 3.4)	27.5–30.3 (28.8 ± 0.9)	27.4–30.5 (28.6 ± 1.1)
6	Dorsal origin to pectoral-fin insertion	27.2–28.7 (27.8 ± 0.8)	30.5–33.2 (32.4 ± 0.8)	29.4–31.8 (30.5 ± 0.9)
7	Dorsal origin to pelvic-fin insertion	24.7–26.6 (25.6 ± 1.0)	29.1–33.6 (31.6 ± 1.4)	25.2–28.3 (26.5 ± 1.2)
8	Dorsal origin to anal-fin origin	39.2–43.6 (41.4 ± 2.2)	43.6–47.8 (46.3 ± 1.2)	40.0–42.6 (41.4 ± 1.0)
9	Dorsal origin to anal-fin insertion	48.8–51.4 (50.0 ± 1.3)	46.3–52.4 (50.6 ± 1.8)	45.9–48.0 (47.2 ± 0.8)
10	Dorsal origin to hypural joint	51.9–55.6 (54.3 ± 2.1)	53.3–56.5 (55.1 ± 1.2)	54.1–56.6 (55.3 ± 1.0)
11	Dorsal origin to adipose-fin origin	40.8–41.6 (41.3 ± 0.4)	41.0–44.0 (42.4 ± 1.0)	39.1–41.2 (40.4 ± 0.7)
12	Length of dorsal-fin base	14.9–17.0 (15.9 ± 1.1)	15.0–17.4 (16.0 ± 0.8)	14.6–15.9 (15.2 ± 0.5)
13	Dorsal-fin insertion to pelvic-fin origin	22.5–24.0 (23.3 ± 0.7)	27.1–30.9 (28.8 ± 1.2)	24.0–25.8 (25.0 ± 0.8)

Table 6. *Continued*

		Leporinus amazonicus	*Leporinus friderici*	*Leporinus klausewitzi*
14	Dorsal-fin insertion to adipose-fin origin	22.5–24.0 (25.7 ± 0.3)	25.8–28.3 (26.9 ± 0.8)	24.0–26.2 (25.2 ± 1.0)
15	Dorsal-fin insertion to anal-fin origin	22.5–24.0 (27.3 ± 1.9)	29.8–33.4 (32.3 ± 1.1)	26.9–29.2 (27.8 ± 0.9)
16	Dorsal-fin insertion to anal-fin insertion	32.5–34.8 (33.5 ± 1.2)	34.0–36.8 (35.7 ± 1.0)	32.1–34.0 (32.9 ± 0.7)
17	Adipose-fin origin to anal-fin origin	14.5–16.7 (15.6 ± 1.1)	17.9–20.9 (19.2 ± 0.9)	16.4–18.0 (17.0 ± 0.6)
18	Adipose-fin origin to anal-fin insertion	10.8–14.7 (12.6 ± 2.0)	13.1–15.3 (14.6 ± 0.6)	10.9–13.2 (12.1 ± 0.9)
19	Adipose-fin origin to hypural joint	10.8–14.7 (13.7 ± 2.0)	11.6–15.7 (14.0 ± 1.3)	13.6–15.7 (14.5 ± 0.7)
20	Length of anal-fin base	9.0–11.8 (10.0 ± 1.6)	9.7–11.1 (10.2 ± 0.5)	9.2–9.9 (9.5 ± 0.3)
21	Anal-fin insertion to hypural joint	10.5–11.2 (10.9 ± 0.3)	8.6–10.3 (9.2 ± 0.5)	10.3–12.3 (11.2 ± 0.7)
22	Pelvic-fin insertion to anal-fin origin	28.5–34.6 (31.0 ± 3.2)	31.6–35.0 (33.2 ± 1.1)	29.4–32.4 (31.1 ± 1.1)
23	Pelvic-fin insertion to adipose-fin origin	40.7–44.1 (41.9 ± 1.9)	40.9–44.7 (43.1 ± 1.3)	38.9–42.3 (40.7 ± 1.3)
24	Pelvic-fin insertion to hypural joint	47.9–53.9 (50.1 ± 3.3)	49.1–51.1 (50.1 ± 0.6)	48.8–52.2 (50.6 ± 1.1)
25	Pelvic-fin insertion to pectoral-fin insertion	20.9–23.8 (22.0 ± 1.6)	24.1–27.5 (25.8 ± 1.2)	22.8–25.4 (23.9 ± 1.2)
26	Greatest body depth	24.7–26.3 (25.7 ± 0.9)	29.2–33.5 (31.8 ± 1.5)	25.4–28.4 (26.6 ± 1.0)
27	Greatest body width	12.4–14.5 (13.4 ± 1.1)	12.7–18.5 (15.3 ± 1.6)	11.8–16.4 (13.2 ± 1.8)
28	Caudal-peduncle depth	9.0–11.0 (9.8 ± 1.1)	10.9–11.8 (11.3 ± 0.3)	9.5–10.8 (10.2 ± 0.5)
29	Head length	28.0–34.0 (30.5 ± 3.1)	26.3–28.2 (27.3 ± 0.7)	26.2–27.1 (26.6 ± 0.3)
30	Preopercle length	72.5–74.3 (73.1 ± 1.0)	77.7–80.0 (78.8 ± 0.8)	74.3–80.1 (77.7 ± 1.9)
31	Snout to anterior margin of eye	34.2–41.1 (36.8 ± 3.7)	37.9–42.1 (39.9 ± 1.4)	36.3–38.5 (37.3 ± 0.8)
32	Head depth	74.3–78.4 (75.9 ± 2.2)	89.8–99.0 (94.8 ± 2.8)	84.0–90.5 (86.9 ± 2.6)
33	Snout depth	40.6–47.2 (43.5 ± 3.3)	48.5–55.2 (52.3 ± 2.3)	48.0–52.3 (50.2 ± 1.7)
34	Jaw length	20.9–24.7 (22.2 ± 2.1)	21.3–24.9 (23.1 ± 1.2)	16.9–20.7 (19.2 ± 1.6)
35	Eye diameter	16.6–27.0 (23.3 ± 5.8)	24.1–29.9 (27.5 ± 2.0)	24.4–29.9 (27.7 ± 2.3)
36	Interorbital width	31.0–42.1 (36.8 ± 5.6)	40.1–46.1 (43.4 ± 1.8)	37.7–42.5 (39.2 ± 1.7)
37	Snout to supraoccipital crest	80.0–85.7 (82.6 ± 2.9)	84.9–94.0 (90.2 ± 2.5)	85.8–96.3 (92.2 ± 4.5)

		Leporinus lebaili	*Leporinus niceforoi* (types)	*Leporinus* cf. *niceforoi*
	Standard length	48.9–95.3 (64.9 ± 21.2)	117.1–128.0 (122.5 ± 7.7)	33.6–158.9 (80.6 ± 44.8)
1	Snout to dorsal-fin origin	50.3–53.5 (52.3 ± 1.4)	44.6–46.1 (45.4 ± 1.0)	45.9–52.1 (48.5 ± 1.4)
2	Snout to adipose-fin origin	85.6–89.4 (87.2 ± 1.7)	84.4–86.7 (85.5 ± 1.7)	83.3–89.6 (86.4 ± 1.9)
3	Snout to anal-fin origin	82.2–84.1 (82.9 ± 0.9)	81.0–81.2 (81.1 ± 0.1)	78.0–86.3 (83.0 ± 2.1)
4	Snout to pelvic-fin insertion	53.0–54.8 (54.2 ± 0.8)	47.0–49.3 (48.1 ± 1.6)	49.2–53.3 (50.7 ± 1.1)
5	Snout to pectoral-fin insertion	30.5–32.5 (31.2 ± 0.9)	24.2–25.8 (25.0 ± 1.2)	25.0–32.1 (28.1 ± 2.5)
6	Dorsal origin to pectoral-fin insertion	32.1–33.9 (33.1 ± 0.9)	26.6–27.4 (27.0 ± 0.6)	23.9–30.5 (28.3 ± 1.8)
7	Dorsal origin to pelvic-fin insertion	31.1–33.7 (32.3 ± 1.2)	20.6–22.7 (21.6 ± 1.5)	22.0–26.6 (24.8 ± 1.1)
8	Dorsal origin to anal-fin origin	43.1–46.2 (44.5 ± 1.5)	42.0–43.6 (42.8 ± 1.2)	39.6–46.9 (43.6 ± 2.2)
9	Dorsal origin to anal-fin insertion	46.8–49.1 (48.4 ± 1.1)	49.1–51.7 (50.4 ± 1.9)	44.6–53.0 (49.5 ± 2.5)
10	Dorsal origin to hypural joint	53.4–54.4 (53.9 ± 0.4)	58.9–60.2 (59.6 ± 0.9)	50.9–59.2 (55.7 ± 2.1)
11	Dorsal origin to adipose-fin origin	36.0–39.9 (38.3 ± 1.7)	44.1–45.4 (44.7 ± 0.9)	36.3–45.1 (41.4 ± 2.6)
12	Length of dorsal-fin base	15.5–16.7 (16.4 ± 0.6)	14.7–14.8 (14.7 ± 0.0)	12.8–17.2 (15.2 ± 1.1)
13	Dorsal-fin insertion to pelvic-fin origin	28.2–30.2 (29.2 ± 0.9)	19.1–20.1 (19.6 ± 0.7)	20.0–25.7 (23.3 ± 1.3)
14	Dorsal-fin insertion to adipose-fin origin	20.4–23.5 (22.4 ± 1.4)	29.1–30.5 (29.8 ± 1.0)	21.4–30.2 (26.3 ± 2.4)
15	Dorsal-fin insertion to anal-fin origin	28.8–30.6 (29.9 ± 0.8)	29.7–29.9 (29.8 ± 0.2)	22.9–33.1 (28.9 ± 2.6)
16	Dorsal-fin insertion to anal-fin insertion	32.1–32.8 (32.4 ± 0.3)	34.1–35.8 (35.0 ± 1.2)	29.2–37.9 (34.2 ± 2.5)
17	Adipose-fin origin to anal-fin origin	19.6–20.8 (20.2 ± 0.5)	13.7–13.7 (13.7 ± 0.1)	13.3–16.8 (15.2 ± 0.9)
18	Adipose-fin origin to anal-fin insertion	15.0–15.6 (15.3 ± 0.3)	10.9–12.2 (11.5 ± 0.9)	10.1–13.4 (12.3 ± 0.8)
19	Adipose-fin origin to hypural joint	13.8–15.6 (14.8 ± 0.8)	17.3–18.0 (17.7 ± 0.5)	10.3–18.7 (13.7 ± 1.7)
20	Length of anal-fin base	8.7–10.9 (10.2 ± 1.0)	6.9–8.2 (7.6 ± 0.9)	7.7–11.7 (9.6 ± 1.1)
21	Anal-fin insertion to hypural joint	9.6–11.1 (10.3 ± 0.6)	10.3–10.9 (10.6 ± 0.4)	7.6–12.6 (9.5 ± 1.3)
22	Pelvic-fin insertion to anal-fin origin	28.2–29.8 (28.9 ± 0.8)	30.4–31.8 (31.1 ± 1.0)	29.5–36.6 (33.0 ± 2.6)
23	Pelvic-fin insertion to adipose-fin origin	38.9–42.9 (41.1 ± 1.8)	39.8–39.8 (39.8 ± 0.0)	46.0–44.0 (39.8 ± 2.3)
24	Pelvic-fin insertion to hypural joint	45.7–48.4 (47.0 ± 1.1)	49.3–52.9 (51.1 ± 2.5)	46.4–53.1 (49.8 ± 1.9)
25	Pelvic-fin insertion to pectoral-fin insertion	21.6–24.6 (23.4 ± 1.3)	23.3–25.2 (24.3 ± 1.3)	20.2–26.2 (24.1 ± 1.9)
26	Greatest body depth	31.9–33.9 (32.9 ± 1.0)	20.2–22.8 (21.5 ± 1.8)	23.3–27.3 (25.2 ± 1.1)
27	Greatest body width	13.6–14.9 (14.1 ± 0.6)	11.5–12.4 (11.9 ± 0.6)	11.6–15.9 (13.5 ± 1.1)
28	Caudal-peduncle depth	11.6–12.0 (11.8 ± 0.2)	8.1–8.8 (8.4 ± 0.5)	8.1–10.7 (9.5 ± 0.7)
29	Head length	27.2–31.7 (29.3 ± 1.8)	23.3–23.9 (23.6 ± 0.5)	23.6–30.4 (26.9 ± 2.4)

Table 6. *Continued*

		Leporinus lebaili	*Leporinus niceforoi* (types)	*Leporinus* cf. *niceforoi*
30	Preopercle length	76.7–82.4 (80.0 ± 2.8)	75.6–77.1 (76.3 ± 1.0)	73.4–80.9 (76.8 ± 2.1)
31	Snout to anterior margin of eye	36.3–40.7 (38.8 ± 2.2)	37.8–40.6 (39.2 ± 2.0)	30.7–42.1 (36.8 ± 3.2)
32	Head depth	91.7–97.9 (95.2 ± 2.9)	74.1–78.1 (76.1 ± 2.8)	61.4–84.4 (73.0 ± 6.6)
33	Snout depth	50.3–56.9 (52.7 ± 2.9)	45.0–45.8 (45.4 ± 0.6)	39.4–50.5 (44.5 ± 3.5)
34	Jaw length	20.0–24.4 (22.5 ± 2.2)	20.9–23.3 (22.1 ± 1.7)	18.0–25.0 (21.7 ± 1.9)
35	Eye diameter	26.4–28.9 (27.3 ± 1.1)	26.6–26.9 (26.7 ± 0.2)	22.6–35.1 (28.6 ± 3.2)
36	Interorbital width	35.1–43.1 (39.3 ± 3.3)	38.7–40.2 (39.4 ± 1.1)	32.2–42.9 (38.1 ± 3.2)
37	Snout to supraoccipital crest	88.1–95.0 (92.1 ± 2.9)	94.4–95.8 (95.1 ± 1.0)	80.6–97.9 (89.7 ± 4.3)

		Leporinus ortomaculatus	*Leporinus* sp.
	Standard length	42.0–78.0 (62.3 ± 11.3)	81.6–115.9 (97.2 ± 16.8)
1	Snout to dorsal-fin origin	46.9–51.6 (48.5 ± 1.3)	47.4–50.1 (49.3 ± 1.1)
2	Snout to adipose-fin origin	83.8–88.0 (85.9 ± 1.2)	87.2–89.1 (88.0 ± 0.8)
3	Snout to anal-fin origin	78.2–83.1 (80.9 ± 1.5)	83.3–86.3 (84.8 ± 1.1)
4	Snout to pelvic-fin insertion	48.9–53.3 (51.7 ± 1.2)	52.5–54.4 (53.3 ± 0.7)
5	Snout to pectoral-fin insertion	26.5–30.3 (28.1 ± 1.1)	27.1–30.1 (28.7 ± 1.3)
6	Dorsal origin to pectoral-fin insertion	24.3–29.5 (27.3 ± 1.6)	27.9–29.7 (29.1 ± 0.7)
7	Dorsal origin to pelvic-fin insertion	21.5–24.8 (23.3 ± 1.0)	22.9–25.3 (23.9 ± 1.0)
8	Dorsal origin to anal-fin origin	28.3–42.7 (41.0 ± 1.4)	40.0–44.4 (42.4 ± 1.6)
9	Dorsal origin to anal-fin insertion	46.4–49.9 (47.7 ± 1.1)	47.8–51.6 (50.3 ± 1.5)
10	Dorsal origin to hypural joint	52.9–57.3 (54.9 ± 1.2)	53.6–57.2 (55.3 ± 1.6)
11	Dorsal origin to adipose-fin origin	37.9–41.4 (39.4 ± 1.0)	39.2–42.1 (40.8 ± 1.2)
12	Length of dorsal-fin base	13.9–16.5 (15.2 ± 0.8)	14.2–14.8 (14.5 ± 0.2)
13	Dorsal-fin insertion to pelvic-fin origin	20.5–23.0 (21.8 ± 0.9)	20.6–23.7 (22.6 ± 1.2)
14	Dorsal-fin insertion to adipose-fin origin	24.1–26.6 (25.2 ± 0.7)	24.3–27.7 (26.4 ± 1.7)
15	Dorsal-fin insertion to anal-fin origin	26.0–28.6 (27.5 ± 0.8)	25.5–29.4 (28.1 ± 1.6)
16	Dorsal-fin insertion to anal-fin insertion	309–34.7 (33.0 ± 1.2)	33.6–34.7 (34.2 ± 0.4)
17	Adipose-fin origin to anal-fin origin	14.5–15.8 (15.0 ± 0.4)	14.1–15.6 (14.6 ± 0.6)
18	Adipose-fin origin to anal-fin insertion	10.7–12.4 (11.7 ± 0.5)	11.3–13.2 (12.2 ± 0.7)
19	Adipose-fin origin to hypural joint	13.0–15.2 (14.3 ± 0.6)	13.7–14.6 (14.1 ± 0.5)
20	Length of anal-fin base	9.5–10.8 (10.0 ± 0.4)	7.8–10.4 (9.1 ± 1.0)
21	Anal-fin insertion to hypural joint	8.9–11.8 (10.0 ± 1.0)	8.1–9.8 (8.8 ± 0.7)
22	Pelvic-fin insertion to anal-fin origin	28.2–33.5 (30.5 ± 1.5)	31.4–34.5 (33.0 ± 1.1)
23	Pelvic-fin insertion to adipose-fin origin	35.5–40.4 (38.3 ± 1.5)	38.5–41.7 (40.4 ± 1.2)
24	Pelvic-fin insertion to hypural joint	43.8–50.9 (47.7 ± 2.0)	47.5–50.5 (48.9 ± 1.1)
25	Pelvic-fin insertion to pectoral-fin insertion	20.0–26.5 (24.1 ± 1.8)	24.1–27.2 (26.2 ± 1.2)
26	Greatest body depth	22.1–25.1 (23.5 ± 1.0)	22.2–25.5 (24.1 ± 1.2)
27	Greatest body width	9.9–13.6 (11.9 ± 1.2)	11.7–14.1 (13.0 ± 0.9)
28	Caudal-peduncle depth	8.2–9.9 (9.1 ± 0.5)	8.7–9.2 (9.0 ± 0.2)
29	Head length	24.2–27.2 (25.5 ± 1.0)	25.1–27.7 (26.1 ± 1.0)
30	Preopercle length	74.2–78.1 (76.8 ± 1.0)	76.6–78.8 (77.9 ± 1.0)
31	Snout to anterior margin of eye	33.5–41.1 (37.8 ± 2.1)	36.4–41.3 (38.8 ± 2.3)
32	Head depth	71.7–81.2 (76.1 ± 2.6)	70.1–76.1 (72.8 ± 2.5)
33	Snout depth	40.7–49.0 (44.7 ± 2.5)	44.6–50.2 (47.5 ± 2.2)
34	Jaw length	17.4–22.6 (20.3 ± 1.3)	21.5–23.7 (22.9 ± 0.9)
35	Eye diameter	25.3–31.2 (28.2 ± 1.9)	23.9–28.0 (26.4 ± 1.6)
36	Interorbital width	32.4–39.3 (35.7 ± 2.0)	33.1–36.8 (35.5 ± 1.6)
37	Snout to supraoccipital crest	92.1–101.2 (95.7 ± 2.9)	87.3–93.9 (91.6 ± 2.6)

Leporinus aff. *cylindriformis*, Mol *et al.* 2007: 365 (historic presence in region now spanned by Brokopondo reservoir, Suriname River drainage, Suriname).

Holotype: SURINAME: Saramacca: FMNH 116827, 111.1 mm, Coppename River, Sidonkrutu, sand island and channel (04°31′51″N, 56°30′56″W) J. Mol, B. Chernoff, P. Willink & M. Cooperman, 9.iii.2004.

Paratypes: SURINAME: Nickerie: USNM 225993, 7 specimens, 68.8–93.6 mm (2 CS, 75.1–89.9 mm); NZCS F-7067 (out of USNM 225993), 1 specimen, 82.3 mm, Corantijn River drainage, Matappi Creek (05°01′N, 57°17.5′W), H. M. Madarie, 17.v.1980. Sipaliwini: MHNG 2672.085, 1 specimen, 113.8 mm; NZCS F-7068 (out of MHNG 2672.085), 1 specimen, 110.8 mm, Corantijn River at Wonotobo Falls, around camp (4°11′0.5″N, 57°57′25.1″W), J. I. Montoya-Burgos, R. Covain & P. Hollanda Carvallo. MHNG 2673.002, 3 specimens, 48.6–127.7 mm, Corantijn River, Kaw Falls (04°59′48.3″N, 57°37′49.5″W), J. I. Montoya-Burgos, R. Covain & P. Hollanda Carvallo. MHNG 2673.083, 1 specimen, 118.0 mm, Gran Rio, Suriname River drainage, at Assigon (3°57′3.9″N, 55°32′1.6″W), J. I. Montoya-Burgos, R. Covain & P. Hollanda Carvallo. MHNG 2673.098, 1 specimen, 133.9 mm, Gran Rio, Suriname River drainage, at Kossindo in front of Cajana village (3°54′5.4″N, 55°34′26.5″W) J. I. Montoya-Burgos, R. Covain & P. Hollanda Carvallo.

Diagnosis: Leporinus apollo can be distinguished from all other members of *Leporinus* except *L. cylindriformis, L. niceforoi, L.* cf. *niceforoi, L. ortomaculatus,* and a possibly undescribed species from the Amazon drainage (*Leporinus* sp., see discussion below) by the combination of an extremely dorsoventrally slender body (percentage of body depth immediately anterior to the dorsal-fin origin in standard length in range of 18–23%) and a pigmentation pattern including three or four large, black spots centred along the lateral-line-scale row. *Leporinus apollo* can be distinguished from *L. niceforoi, L. ortomaculatus,* and *Leporinus* sp. by the possession of six scales in a transverse series above the lateral line (in all but one examined specimen, which has five scales in that series) versus five scales in that series in all examined specimens of *L. niceforoi, L. ortomaculatus,* and *Leporinus* sp. It can be distinguished from *L.* cf. *niceforoi* by the percentage of body depth in standard length of 18.3–22.9% versus 23.3–27.3% and by the typical transverse scale count at the dorsal and pelvic fin origins of 6/5 (5/5 and 6/4 each occur once) versus a typical count of 5/4 (occasionally 5/5, once 6/4, never 6/5). *Leporinus apollo* can be distinguished from *L. cylindriformis* and *L. niceforoi* by the presence of a small, dark spot on the body immediately ventral to the seventh, eighth, or ninth scale of the lateral line, versus the absence of such a spot in those two species. *Leporinus apollo* can be further distinguished from *L. cylindriformis* by the possession of a dark spot centred immediately posterior to the opercle and slightly ventral to the lateral-line-scale row (versus the lack of such a spot), the presence of a series of nine to 14 dark bars across the dorsal surface of the body that terminate ventrally in

darker areas that form an irregular stripe situated dorsal and parallel to the lateral line scale row (versus the lack of well-developed transverse bars and absence of such dark areas), and by the percentage of body width in standard length in the range of 9.7–14.0% (versus 15.2%).

Description: Meristic counts for holotype and paratypes in Table 5, morphometrics in Table 6. Body fusiform and very slender, with body depth 18.3–22.9% of SL. Head elongate and roughly triangular in lateral profile, with depth measured at posterior terminus of opercle 62.7–72.3% of head length. Greatest depth and width of body located at vertical through dorsal-fin origin. Profile of predorsal region of body nearly straight, with only slight convexity. Dorsal fin-base and profile of body from base of last dorsal-fin ray to adipose fin straight and posteroventrally slanted. Body with distinct vertical constriction in region posterior of adipose fin and anterior of hypural plate. Adipose-fin origin located on vertical through base of fourth branched anal-fin ray. Ventral margin of head and body straight and posteroventrally inclined from tip of lower jaw to inflection point directly ventral to dorsal-fin origin. Ventral profile of body posterodorsally angled posterior to that point. Pelvic-fin insertion located at vertical through base of second branched dorsal-fin ray.

Mouth small and slightly subterminal; upper and lower jaws meet along horizontal tangent to ventral margin of eye. Ventral margin of upper jaw sinusoidal, reflecting oblique angle between ventral margin of premaxilla and maxilla. Margins of upper and lower lips with slight ridges. Premaxilla and maxilla each typically bear four teeth. Teeth on each jaw graded in size with symphyseal teeth largest and terminal tooth of series distinctly smaller. Single row of replacement teeth present in crypt within dentary. Dentary teeth fit far behind teeth of upper jaw in closed mouth, resulting in pronounced overbite.

Anterior nare tubular and anteriorly directed. Posterior nare rhomboidal or in shape of figure of eight, with approximately ten olfactory ridges visible externally. Nares situated on horizontal bisecting ventral hemisphere of pupil. Antorbital, infraorbitals, and supraorbital with general forms comparable to that illustrated for *L. fasciatus* in Sidlauskas & Vari (2008: fig. 9) other than for a wider nasal and for the fusion of the fourth and fifth infraorbitals into a single element with posteriorly directed branch of laterosensory canal midway along its vertical extent.

Four branchiostegal rays with medial ray smallest. Fleshy opercular membrane fused to isthmus.

Anal fin preceded by single very small additional unbranched ray, visible in radiographs but not externally and not included in counts. First externally

visible unbranched ray of anal fin one-half or less length of second unbranched ray. Branched rays of anal fin articulated to second to ninth proximal and distal pterygiophores. Dorsal fin preceded by single very small additional unbranched ray, visible in radiographs but not externally and not included in counts. First externally visible unbranched ray of dorsal fin slightly more than one-half length of second unbranched dorsal-fin ray. Branched rays of dorsal fin articulated to second through 11th proximal and distal pterygiophores. First dorsal pterygiophore typically lies between neural processes of 11th and 12th or tenth and 11th vertebrae, but in one individual between neural processes of ninth and tenth vertebrae.

Pectoral fin elongate, with second and third unbranched rays longest. Adipose fin elongate with convex upper margin and straight or concave ventral margin. Caudal-fin lobes distinctly pointed, with longest rays those immediately ventral to dorsalmost rays and immediately dorsal to ventralmost rays.

Body fully scaled. Fins not scaled except for row of small scales at base of anal fin and overlaying basal portion of middle caudal-fin rays.

Coloration in alcohol: Overall ground colour pale yellow to light brown, darkest dorsal to lateral line and palest on ventral surface of head, gular region and portion of body ventral to third scale row below lateral-line scale row. Dorsal surface of head, upper jaw, and area lateral to infraorbital series dusky. Skin covering upper margin of maxilla distinctly darker than skin covering remainder of maxilla, resulting in pigmentation in the form of thin moustache.

Four large dark spots ranging in shape from circular to horizontally elongate ellipses located along lateral surface of body. Anterior spot centred on first scale row ventral to lateral-line-scale row and posterior three spots centred on lateral-line scale row. First large spot begins just posterior to fleshy flap of opercle and extends posteriorly across approximately three scales. Anterior limit of second large spot situated at vertical through base of second branched dorsal-fin ray, with spot extending posteriorly across six or seven scales. Anterior limit of third large spot located immediately posterior to vertical through posterior limit of anus, with spot extending posteriorly across approximately five scales. Fourth large spot centred over caudal peduncle, spanning approximately five scales.

Variable number of small accessory spots positioned along second or third horizontal scale row ventral to lateral-line scale row. All examined specimens with at least one such small spot centred on second horizontal scale row below lateral-line scale row and located ventral to seventh, eighth, or ninth lateral line scale.

Most specimens with additional small spot located midway between and slightly ventral to second and third large spots (this spot absent in all three specimens in MHNG 2673.002, see Fig. 2). Some specimens (MHNG 2673.083, MHNG 2673.098) with as many as seven additional small spots arranged in irregular horizontal line across ventrolateral portion of body.

Nine to 14 (typically 13 or 14) dark transverse bars extending across dorsal surface of body, each terminating on left and right side in area of more intense dark pigmentation positioned over third (anteriorly) or second (posteriorly) horizontal scale row dorsal to lateral-line-scale row. Contrast between transverse dorsal bars and ground coloration typically pronounced, but some specimens (MHNG 2672.085, NZCS F-7068) with pigmentation of dorsal transverse bars muted and less intense. Rayed fins hyaline except for widely dispersed melanophores outlining caudal-fin rays. Adipose fin pale overall, but occasionally with dusky border.

Coloration in juveniles (two smallest specimens in MHNG 2673.002, both measuring approximately 49 mm SL) similar overall to pigmentation in adults, with four large lateral spots, transverse dorsal bars, and horizontal series of smaller spots dorsal and ventral to lateral-line-scale row all in evidence. Second and third large lateral spots extend further ventrally in juveniles than in adults, with dark pigmentation in juveniles approaching, but not contacting, bases of pectoral and anal fins.

Coloration in life: Based upon two photographs taken immediately after capture and kindly provided by R. Covain: ground colour pale yellow, with pectoral and pelvic fins and exposed portions of interopercle and subopercle displaying more intensely yellow coloration. Margin of adipose fin orange or red. Pigmentation otherwise as described for preserved material.

Growth and ontogeny: Small to moderate sized species of *Leporinus*, with maximum known body size of 133.9 mm SL. Juveniles with proportionally larger heads than adults, with percentage of head length in SL about 23% in smallest specimens (~49 mm SL) and about 26% in largest specimens. Slightly subterminal mouth position invariant amongst examined specimens, although an ontogenetic shift in mouth position may occur in very small juveniles as it does in many other members of the Anostomidae (Santos, 1980; Sidlauskas *et al*., 2007).

Geography: Known only from the Coppename, Corantijn, and Suriname rivers of western and central Suriname (Fig. 12), which flow from the Guyana Shield into the Atlantic Ocean. The historic distribu-
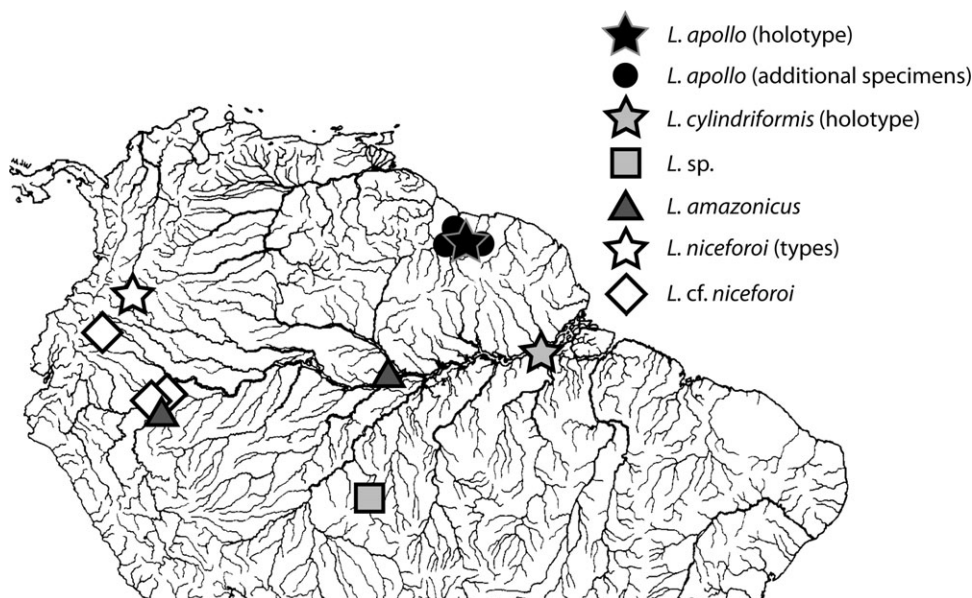
Figure 12. Geographical distribution of examined specimens of *Leporinus amazonicus*, ***Leporinus apollo* sp. nov.**, *Leporinus cylindriformis*, *Leporinus niceforoi*, *Leporinus* cf. *niceforoi*, and *Leporinus* sp. Some symbols represent more than one collection locality.

tion included the region of the Suriname river currently spanned by the Brokopondo reservoir, as two specimens were collected there in 1963–64 prior to the closure of the dam and the creation of the reservoir (Mol *et al.*, 2007, listed as *L.* aff. *cylindriformis* in their appendix 1) Extensive subsequent collections in Brokopondo have yielded no additional specimens of *L. apollo*, suggesting that it is now extirpated from the reservoir (Mol *et al.*, 2007).

Phylogenetic placement: Dissection of the CS specimens of *L. apollo* reveals the species to lack the synapomorphies of *Hypomasticus* (clade 4 of Sidlauskas & Vari, 2008), but to possess instead a character distribution that would nest the species within clade 8 of the phylogeny advanced in that publication. As *L. apollo* also lacks the synapomorphies of Sidlauskas & Vari's (2008) clade 12 (which contains the majority of genera within the Anostomidae that nest within clade 8) it clearly fits within the current concept of *Leporinus*.

Etymology: We name the species 'apollo' after the god of the sun, music and healing in Greek and Roman mythology. The extremely slender form of the new species is reminiscent of the arrow that was Apollo's favoured weapon and predominant symbol, and the yellow cast of the body and fins and the rounded shape of the lateral markings evoke the sun that was one of Apollo's primary aspects.

Comparison with Leporinus gossei: As noted by Willink & Sidlauskas (2006), *L. apollo* has a very similar colour pattern to that of *L. gossei*, a rare species known solely from French Guiana (see photograph in Planquette, Keith & Le Bail, 1996: 155). Although no specimens of *L. gossei* were available for study, *L. gossei* is clearly a much deeper bodied species than is *L. apollo*. The meristics reported for the two species are also highly dissimilar, with six scales in the upper transverse series and 40–43 total lateral-line scales in *L. apollo* versus four (rarely five) upper transverse scales and 36–37 (rarely 38–39) lateral-line scales in *L. gossei*. Notwithstanding the geographical proximity of the two species, there is no question that *L. gossei* belongs to the assemblage of species centred on *L. friderici* and that *L. gossei* and *L. apollo* are distinct.

Remarks on differentiation from Leporinus cylindriformis: Despite their similarity in meristics and most morphometrics, the coloration of *L. apollo* differs substantially from the current pigmentation of the *L. cylindriformis* holotype and from the original illustration of that specimen, which was prepared around 1870 on behalf of Agassiz and reproduced by Borodin (1929). In particular, the Suriname material possesses a dark mark behind the opercle, another mark ventral to approximately the eighth scale of the lateral line, and many dark bands across the dorsal surface of the body that terminate ventrally in yet darker areas. None of those dark marks appear in the

original drawing of the holotype. Comparison of the coloration in the Suriname material with the holotype itself is complicated by the 150 + years since the preservation of the specimen, which is now rather faded. Although the three horizontally elongate spots along the lateral line scale row that appear in Borodin (1929) can still be seen clearly on the holotype (Fig. 1), these are less extensive than the marks in comparable locations in *L. apollo*. More significantly, the *L. cylindriformis* holotype (Fig. 1) and the original illustration (Borodin, 1929: pl. 10) lack several of the other prominent dark marks present in *L. apollo*. Most notably, there is definitely no dark spot below the eighth scale of the lateral line in the *L. cylindriformis* holotype, and this spot represents the most diagnostic aspect of coloration separating the holotype from the Suriname specimens.

Although the holotype definitely does not currently have the prominent markings that characterize *L. apollo*, the possibility exists that it did at an earlier point in ontogeny. The *L. cylindriformis* holotype at 188.0 mm SL is approximately 45 mm longer than the largest known specimen of *L. apollo* (133.9 mm SL), and thus the apparent differences in coloration might diagnose different developmental stages of the same species, not separate species. Such a scenario would require the loss of a very considerable amount of pigment over a fairly short interval of growth. Given that the largest examined specimens of *L. apollo* are as darkly pigmented as the smallest, we consider this scenario to be highly unlikely. Unfortunately, a search of several museums has revealed no additional material of *L. cylindriformis* that could clarify the issue.

Identification of the material described herein as *L. apollo* as *L. cylindriformis* would also require explanation of the disjunct distribution of the species in the Amazon and in three of the coastal drainages of Suriname, without that species also occurring in Brazil's Amapá state or in French Guiana. Such a geographical distribution is not entirely implausible and could result from vicariance, dispersal via the Amazonian freshwater plume (Muller-Karger, McClain & Richardson, 1988; Hu *et al.*, 2004), or local extinction in the intermediate drainages. Although such a distribution is not impossible, this would be a novel biogeographical pattern; amongst the fish species that have been critically reviewed in recent years we are not aware of any that are distributed in Suriname and the central Amazon without intervening populations. Taken as a whole, the scenario of synonymy is significantly more convoluted than the alternative that *L. apollo* represents a new species closely allied to *L. cylindriformis*.

As a final enigma, the absence of additional specimens of *L. cylindriformis* begs explanation. Is the species naturally rare or an inhabitant of rarely sampled habitats such as rapids? Does the specimen represent a species that is now extirpated in the vicinity of Porto de Moz? If so, might a population still exist elsewhere, perhaps further upriver along the Rio Xingu? The possibilities are numerous, but any answers must remain speculative unless new specimens are discovered in a museum collection or in the vastness of the Amazon.

LEPORINUS CYLINDRIFORMIS OF RECENT YEARS: NOT WHAT WAS THOUGHT

The holotype of *L. cylindriformis* clearly does not match the series of specimens assigned to that species by Santos & Zuanon (2008), which are referred herein to *Leporinus* sp. Both linear and geometric methods revealed the *L. cylindriformis* holotype to have a shallower body than does *Leporinus* sp. (Figs 6, 11). The *L. cylindriformis* holotype falls well outside the 95% confidence ellipse for *Leporinus* sp. in the scatterplot of PC2 versus PC1 from the geometric analysis. Furthermore, the *L. cylindriformis* holotype has six scales in the transverse series above the lateral line, whereas all examined specimens of *Leporinus* sp. have five scales in that series.

It is important to note that the lot of *Leporinus* sp. examined in this study (INPA 15405) does not appear in the series of comparative material that Santos & Zuanon (2008) assigned to *L. cylindriformis* during their description of *L. amazonicus*, presumably because it was on loan to us at the time that they prepared their manuscript. The lot that we examined is from the same general region of Brazil as Santos & Zuanon's (2008) specimens (Fig. 12) and it was originally identified by staff at INPA as *Leporinus cylindriformis*. There is no doubt that Santos & Zuanon's (2008) concept of *L. cylindriformis* matches the *Leporinus* sp. of this contribution.

Although *Leporinus* sp. clearly does not belong to the same species as the *L. cylindriformis* holotype, its taxonomic status is unresolved. It might represent an undescribed species, but it is morphometrically (Tables 2–4) and meristically (Table 5) indistinguishable from *L.* cf. *niceforoi* despite inhabiting a separate region of the Amazon drainage. These two groups also share similar colour patterns. If *Leporinus* sp. is conspecific with all, or part of, the current concept of *L. niceforoi*, this would represent a major range extension for *L. niceforoi*. Many more specimens from a broader geographical range are required to resolve this question. Until such specimens are available, we prefer to put the taxonomic status of *Leporinus* sp. into abeyance.

LEPORINUS NICEFOROI: ONE SPECIES OR TWO?

Surprisingly, traditional linear morphometrics suggest that the holotype and paratype of *L. niceforoi*

from Colombia are separable from putative conspecifics from Ecuador and Peru (*L.* cf. *niceforoi*) on the basis of the more slender bodies in the two Colombian specimens. These type specimens fall well outside the range of *L.* cf. *niceforoi* on the PC2 from traditional morphometrics (Fig. 6), and Tukey's post-hoc test on the PC2 scores returned a *P*-value of 0.0001 for separation of these two groups (Table 3). Indeed, simple examination of the ratios of body depth in standard length (Table 6) reveals that the types of *L. niceforoi* fall within the range of *L. apollo* and *L. cylindriformis*, which are the two most dorsoventrally slender examined species in the genus. As only the two type specimens of *L. niceforoi* are available, the regression-based test for variation in the intercept of the linear PC1 as reported in Table 2 cannot be performed for this group. Furthermore, because the specimens are bent, these specimens cannot be included in the geometric morphometric analysis. Other than the morphometric difference and the slight geographical separation (Fig. 12), *L.* cf. *niceforoi* and *L. niceforoi* have identical colour patterns and meristic counts (Table 5).

Although the presence of two cryptic species within the current concept of *L. niceforoi* is a possible explanation for the described differences in body depth, at least two other scenarios are possible. First, a morphocline may exist within this species, which would be revealed by the incorporation of more extensive geographical samples of specimens. Second, the type specimens may have shrunk over the course of more than 70 years of storage (Buchheister & Wilson, 2005; Thorstad *et al.*, 2007). Only the examination of recently collected material from at or near the type locality in Colombia complemented by additional samples from Peru and Ecuador will resolve these questions.

GEOGRAPHICAL AND DEVELOPMENTAL NOTE ON L. AMAZONICUS

Santos & Zuanon (2008) described *L. amazonicus* from a small series of adult specimens collected near Manaus, Brazil. In their discussion Santos & Zuanon noted that the species appears to be rare near Manaus, and that those collections might be from the margin of the species' distribution. We were able to locate only three specimens of *L. amazonicus* in North American collections, suggesting that it is indeed quite rare. Importantly, one of our three examined specimens (UF 162283, an adult from the Río Ucayali, Peru) represents a major range extension for the species. The record suggests that *L. amazonicus* may occur throughout the upper and central Amazon basin. The other two specimens (USNM 305164 and USNM 305230, both from near Manaus) are much

smaller than the material examined by Santos & Zuanon (63.6 and 25.2 mm SL, respectively) and demonstrate that the single dark lateral spot that characterizes *L. amazonicus* is present in juveniles as well as adults of the species.

REFERENCES

Adams DC, Rohlf FJ, Slice DE. 2004. Geometric morphometrics: ten years of progress following the 'revolution'. *Italian Journal of Zoology* **71:** 5–16.

Birch JM. 1997. Comparing wing shape of bats: the merits of principal-components analysis and relative-warp analysis. *Journal of Mammalogy* **78:** 1187–1198.

Bloch ME. 1794. *Naturgeschichte der ausländischen Fische*, Vol. 8. Berlin.

Bookstein FL. 1991. *Morphometric tools for landmark data*. Cambridge: Cambridge University Press.

Bookstein FL, Chernoff B, Elder RL, Humphries JM, Smith GR, Strauss RE. 1985. *Morphometrics in evolutionary biology: the geometry of size and shape change*, Vol. 15. Philadelphia, Pennsylvania: Academy of Natural Sciences.

Borodin NA. 1929. Notes on some species and subspecies of the genus *Leporinus* Spix. *Memoirs of the Museum of Comparative Zoology* **50:** 269–290, pls. 261–217.

Britski HA, Birindelli JLO. 2008. Description of a new species of the genus *Leporinus* Spix (Characiformes: Anostomidae) from the rio Araguaia, Brazil, with comments on the taxonomy and distribution of *L. parae* and *L. lacustris*. *Neotropical Ichthyology* **6:** 45–51.

Britski HA, Garavello JC. 2005. Uma nova espécie de *Leporinus* Agassiz, 1829, da bacia Amazônica (Ostariophysi: Characiformes: Anostomidae). *Comunicações do Museu de Ciências e Tecnologia da PUCRS, Séries Zoologia, Porto Alegre* **18:** 75–83.

Buchheister A, Wilson MT. 2005. Shrinkage correction and length conversion equations for *Theragra chalcogramma, Mallotus villosus* and *Thaleichthys pacificus*. *Journal of Fish Biology* **67:** 541–548.

Burnaby TP. 1966. Growth-invariant discriminant functions and generalized distances. *Biometrics* **22:** 96–110.

Chernoff B, Machado-Allison A. 1999. *Bryconops colaroja* and *B. colanegra*, two new species from the Cuyuni and Caroni drainages of South America (Teleostei: Characiformes). *Ichthyological Exploration of Freshwaters* **10:** 355–370.

Chernoff B, Machado-Allison A. 2005. *Bryconops magoi* and *Bryconops collettei* (Characiformes: Characidae), two new freshwater fish species from Venezuela, with comments on *B. caudomaculatus* (Günther). *Zootaxa* **1094:** 1–23.

Cuvier G. 1816. *La règne animal distribué d'après son organisation pour servir de base à histoire naturelle des animaux et d'introduction à l'anatomie comparée les reptiles, les poissons, les mollusques et les annélides*, 1st edn, Vol. 2.

Cuvier G, Valenciennes A. 1850. *Histoire naturelle des poissons. Tome vingt-deuxième. Suite du livre vingt-deuxième. Suite de la famille des Salmonoïdes*, Vol. 22, pp. xx + 1 + 532 + 91p., pls 634–650. Paris and Strasbourg: Ch. Pitois, & V. Levrault.

Dryden IL, Mardia KV. 1998. *Statistical shape analysis*. New York: John Wiley & Sons.

Fernandes CC, Lundberg JG, Riginos C, McEachran JD. 2002. Largest of all electric-fish snouts: hypermorphic facial growth in male *Apteronotus hasemani* and the identity of *Apteronotus anas* (Gymnotiformes: Apteronotidae). *Copeia* **2002:** 52–61.

Fink WL. 1993. Revision of the piranha genus *Pygocentrus* (Teleostei, Characiformes). *Copeia* **1993:** 665–687.

Fink WL, Weitzman SH. 1974. The so-called cheirodontin fishes of Central America with descriptions of two new species (Pisces: Characidae). *Smithsonian Contributions to Zoology* **172:** 1–46.

Fink WL, Zelditch ML. 1995. Phylogenetic analysis of ontogenetic shape transformations: a reassessment of the piranha genus *Pygocentrus* (Teleostei). *Systematic Biology* **44:** 343–360.

Fink WL, Zelditch ML. 1997. Shape analysis and taxonomic status of *Pygocentrus* piranhas (Ostariophysi, Characiformes) from the Paraguay and Paraná river basins of South America. *Copeia* **1997:** 179–182.

Fowler HW. 1943. A collection of fishes from Colombia, obtained chiefly by Brother Nicéforo Maria. *Proceedings of the Academy of Natural Sciences of Philadelphia* **95:** 223–266.

Garavello JC. 2000. Two new species of Leporinus Spix with a review of the blotched species of the Rio Orinoco system and rescription of Leporinus muyscorum Steindachner (Characiformes: Anostomidae). *Proceedings of the Academy of Natural Sciences of Philadelphia* **150:** 193–201.

Géry J. 1960. Contributions to the study of the characoid fishes No. 9. Some South-American characoid fishes in the Senckenberg Museum, with the description of a new *Leporinus*. *Senckenbergiana Biologica* **41:** 273–288.

Gould SJ. 1971. Geometric similarity in allometric growth: a contribution to the problem of scaling in the evolution of size. *The American Naturalist* **105:** 113.

Günther A. 1864. *Catalogue of the fishes in the British Museum, Vol. 5. Catalogue of the Physostomi, containing the families Siluridae, Characinidae, Haplochitonidae, Sternoptychidae, Scopelidae, Stomiatidae in the collection of the British Museum*. London.

Hammer Ø, Harper DAT, Ryan PD. 2001. PAST: paleontological statistics software package for education and data analysis. *Palaeontologia Electronica* **4:** 1–9.

Harvey PH, Pagel M. 1991. *The comparative method in evolutionary biology*. Oxford: Oxford University Press.

Hotelling H. 1935. The most predictable criterion. *Journal of Educational Psychology* **26:** 139–142.

Hu C, Montgomery ET, Schmitt RW, Muller-Karger FE. 2004. The dispersal of the Amazon and Orinoco River water in the tropical Atlantic and Caribbean Sea: observation from space and S-PALACE floats. *Deep Sea Research Part II: Topical Studies in Oceanography* **51:** 1151–1171.

Hubbs CL, Bailey RM. 1940. A revision of the black basses (Micropterus and Huro) with descriptions of four new forms. *Miscellaneous Publications of the Museum of Zoology, University of Michigan* **48:** 1–51 + 56 plates, 52 maps.

Hubbs CL, Lagler KF. 1958. *Fishes of the Great Lakes region*, Vol. 26. Bloomfield Hills, MI: Cranbrook Institute of Science.

Hubbs CL, Lagler KF. 2004. *Fishes of the Great Lakes region*, revised edition, revised by Gerald R. Smith. Ann Arbor, MI: The Unversity of Michigan Press, 276.

Humphries JM, Bookstein FL, Chernoff B, Smith GR, Elder RL, Poss SG. 1981. Multivariate discrimination by shape in relation to size. *Systematic Zoology* **30:** 291–308.

Huxley J. 1932. *Problems of relative growth*. London: Methuen.

Jolicoeur PJ. 1963. The multivariate generalization of the allometric equation. *Biometrics* **19:** 497–499.

Kimmel CB, Sidlauskas B, Clack JA. 2009. Linked morphological changes during palate evolution in early tetrapods. *Journal of Anatomy* **215:** 91–109.

Klingenberg CP. 2008. *MorphoJ*. 1.02b ed. Manchester, UK: Faculty of Life Sciences, University of Manchester.

Maderbacher M, Bauer C, Herler J, Postl L, Makasa L, Sturmbauer C. 2008. Assessment of traditional versus geometric morphometrics for discriminating populations of the *Tropheus moorii* species complex (Teleostei: Cichlidae), a Lake Tanganyika model for allopatric speciation. *Journal of Zoological Systematics and Evolutionary Research* **46:** 153–161.

Marr JC. 1955. The use of morphometric data in systematic, racial and relative growth studies in fishes. *Copeia* **1955:** 23–31.

Miller RJ. 1963. Comparative morphology of three cyprinid fishes: *Notropis cornutus, Notropis rubellus*, and the hybrid, *Notropis cornutus* X *Notropis rubellus*. *American Midland Naturalist* **69:** 1–33.

Mol JH, Mérona B, Ouboter PE, Sahdew S. 2007. The fish fauna of Brokopondo Reservoir, Suriname, during 40 years of impoundment. *Neotropical Ichthyology* **5:** 351–368.

Morton WM, Miller RR. 1954. Systematic position of the lake trout, *Salvelinus namaycush*. *Copeia* **1954:** 116–124.

Müller J, Troschel FH. 1845. *Horae Ichthyologicae. Beschreibung und Abbildung neuer Fische. Die Familie der Characinen. Horae Ichthyologicae. Beschreibung und Abbildung neuer Fische. Die Familie der Characinen*, Vol. 1 & 2, 1–40.

Müller J, Troschel FH. 1848. *Fische Reisen in Britisch-Guiana in den Jahren 1840-44. Im Auftrag Sr. Mäjestat des Königs von Preussen ausgeführt von Richard Schomburgk. [Versuch einer Fauna und Flora von Britisch-Guiana.].* Berlin, 618–644.

Müller J, Troschel FH. 1849. *Horae Ichthyologicae. Beschreibung und Abbildung neuer Fische. Berlin. Horae Ichthyologicae. Beschreibung und Abbildung neuer Fische. Die Familie der Characinen*, Vol. 3, 1–27 + additional p. 24.

Muller-Karger FE, McClain CR, Richardson PL. 1988. The dispersal of the Amazon's water. *Nature* **333:** 56–59.

Nunn CL, Barton RA. 2000. Allometric slopes and independent contrasts: a comparative test of Kleiber's Law in primate ranging patterns. *The American Naturalist* **156:** 519–533.

Parsons KJ, Robinson BW, Hrbek T. 2003. Getting into shape: an empirical comparison of traditional truss-based morphometric methods with a newer geometric method applied to new world cichlids. *Environmental Biology of Fishes* **67:** 417–431.

Planquette P, Keith P, Le Bail PY. 1996. *Atlas des poissons d'eau douce de Guyane (tome 1)*, Vol. 22. Paris: Institut d'Ecologie et de Gestion de la Biodiversité – Muséum National d'Histoire Naturelle, Institut National de la Recherche Agronomique, Conseil Supérieur de la Pêche, Ministere de l'Environnement.

Rice WR. 1989. Analyzing tables of statistical tests. *Evolution* **43:** 223–225.

Rincon PA. 2000. Big fish, small fish: still the same species. Lack of morphometric evidence of the existence of two sturgeon species in the Guadalquivir river. *Marine Biology* **136:** 715–723.

Rohlf FJ. 1993. Relative warp analysis and an example of its application to mosquito wings. In: Marcus LF, Bello E, Garcia-Valdecasas A, eds. *Contributions to morphometrics*. Madrid: Museo Nacional de Ciencias Naturales, 132–159.

Rohlf FJ. 1996. Morphometric spaces, shape components and the effects of linear transformations. In: Marcus LF, ed. *Advances in morphometrics*. Stony Brook, New York: SUNY (State University of New York), 117–129.

Rohlf FJ. 2006. *Tpsdig*, v 2.10. Stony Brook, NY: SUNY.

Rohlf FJ, Marcus LF. 1993. A revolution in morphometrics. *Trends in Ecology & Evolution* **8:** 129–132.

Rohlf FJ, Slice D. 1990. Extensions of the Procrustes method for the optimal superimposition of landmarks. *Systematic Zoology* **39:** 40–59.

Sabaj Pérez MH. 2010. Standard symbolic codes for institutional resource collections in herpetology and ichthyology: an online reference. Version 2.0 (8 November 2010). Electronically accessible at http://www.asih.org/, American Society of Ichthyologists and Herpetologists, Washington, DC.

Santos GMd. 1980. Aspectos de sistemática e morfologia de *Schizodon fasciatus* Agassiz 1829, *Rhytiodus microlepis* Kner 1859 e *Rhytiodus argenteofuscus* Kner, 1829 (Osteichthyes, Characoidei, Anostomidae) do lago Janauacá-Amazonas. *Acta Amazonica* **10:** 635–649.

Santos GMd, Zuanon J. 2008. *Leporinus amazonicus*, a new anostomid species from the Amazon lowlands, Brazil (Osteichthyes: Characiformes). *Zootaxa* **1815:** 35–42.

Sheets HD. 2004. *Integrated morphometrics package (imp)*. Buffalo: Canisius College. Available at http://www3.canisius.edu/~sheets/morphsoft.html

Sidlauskas B, Chernoff B, Machado-Allison A. 2006. Geographic and environmental variation in *Bryconops* sp. cf. *melanurus* (Ostariophysi: Characidae) from the Brazilian Pantanal. *Ichthyological Research* **53:** 24–33.

Sidlauskas B, Garavello JC, Jellen J. 2007. A new *Schizodon* (Characiformes: Anostomidae) from the Río Orinoco system, with a redescription of *S. isognathus* from the Rio Paraguay system. *Copeia* **2007:** 711–725.

Sidlauskas B, Vari RP. 2008. Phylogenetic relationships within the South American fish family Anostomidae (Teleostei, Ostariophysi, Characiformes). *Zoological Journal of the Linnean Society* **154:** 70–210.

Stevens JP. 2002. *Applied multivariate statistics for the social sciences*. Mahwah, NJ: Lawrence Erlbaum Associates.

Taylor WR, Van Dyke GC. 1985. Revised procedures for staining and clearing small fishes and other vertebrates for bone and cartilage study. *Cybium* **9:** 107–119.

Teissier G. 1936. Croissance comparee des formes locales d'une meme espece. *Mémoires Du Musée Royal Histoire Naturelle Belgique (2nd series)* **3:** 627–634.

Thorstad EB, Finstad AG, Jensen AJ, Museth J, Næsje TF, Saksgård LM. 2007. To what extent does ethanol and freezing preservation cause shrinkage of juvenile Atlantic salmon and European minnow? *Fisheries Management and Ecology* **14:** 295–298.

Turner GF, Pitcher TJ, Grimm AS. 1989. Identification of the Lake Malawi *Oreochromis* (*Nyasalapia*) spp. using multivariate morphometric techniques. *Journal of Fish Biology* **35:** 799–812.

Warton DI, Wright IJ, Falster DS, Westoby M. 2006. Bivariate line-fitting methods for allometry. *Biological Reviews* **81:** 259–291.

Weinberg SL, Darlington RB. 1976. Canonical analysis when number of variables is large relative to sample size. *Journal of Educational and Behavioral Statistics* **1:** 313–332.

Whitlock MC, Schluter D. 2009. *The analysis of biological data*. Greenwood Village, Colorado: Roberts and Company, 393–430.

Willink PW, Sidlauskas B. 2006. Taxonomic notes on select

fishes collected during the 2004 AquaRAP expedition to the Coppename River, Central Suriname Nature Reserve, Suriname. In: Alonso LE, Berrenstein HJ, eds. *A rapid biological assessment of the aquatic ecosystems of the Coppename River Basin, Suriname. RAP Bulletin of Biological Assessment 39*. Washington, DC: Conservation International, 101–111.

Winterbottom R. 1980. Systematics, osteology and phylogenetic relationships of fishes of the ostariophysan subfamily Anostominae (Characoidei, Anostomidae). *Life Sciences Contributions: Royal Ontario Museum* **123:** 1–112.

APPENDIX

MATERIAL EXAMINED

Leporinus amazonicus Santos & Zuanon – Brazil, Amazonas: USNM 305164, 1 specimen, 63.6 mm; USNM 305230, 1 specimen, 25.2 mm: Ilha de Marchantaria. Peru, Loreto: UF 162283, 1 specimen, 170.7 mm, Río Ucayali drainage, Caño Yarina, Pacaya Samiria National Reserve, flooded forest (5°22′0″S, 74°30′48″W).

Leporinus cylindriformis Borodin – Brazil, Pará: MCZ 20430, holotype, 188.0 mm, Rio Xingu at Porto de Moz. (1°45′S, 52°10′W).

Leporinus friderici (Bloch) – Suriname: Nickerie: USNM 225412, 10 specimens, 91.5–148.3 mm, Corantijn River drainage, small stream behind Kamp Infrastructure (opposite Avanavero Airfield).

Leporinus klausewitzi Géry – Venezuela, Amazonas: ANSP 159349, 1 specimen, 88.3 mm, small caño *c*. 5 km below Raudal Peresa, Río Autana (04°46′N, 67°19′W). ANSP 159353, 4 specimens, 62.4–75.6 mm, caño entering Río Sipapo at Raudal del Caldero, *c*. 3 km above confluence with Río Orinoco. ANSP 161703, 1 specimen, 132.3 mm, Caño Caripo, first right caño off Río Casiquiare *c*. 5 min by boat from origin of Río Casiquiare from Río Orinoco (03°06′N, 65°50′W).

Leporinus lebaili Géry and Planquette – Suriname, Sipaliwini: ANSP 189011, 1 specimen, 63.7 mm, Litani River at mouth and confluence with Marowini River, just upstream from settlement of Konya Kondre (03°17′24″N, 54°04′38″W). ANSP 189043, 23 specimens, 48.9–95.3 mm, Lawa River (Marowijne River drainage), base camp *c*. 8 km south-south-west of Anapaike/Kawemhakan airstrip (03°19′31″N, 54°03′48″W).

Leporinus niceforoi Fowler – Colombia, Caqueta: ANSP 70491, holotype, 128.0 mm; ANSP 70492, paratype, 117.1 mm; Florencia, Rio Orteguasa basin, Amazon watershed.

Leporinus cf. *niceforoi* Fowler – Ecuador, Napo: FMNH 102150, 2 specimens, 33.6–75.3 mm, Río Yasuni, 1–2 km downstream from confluence with Rio Jatuncocha (0°59′6″S, 75°25′36″W). FMNH 102153, 6 specimens, 35.4–101.9 mm, Río Tiputini, near mouth in Río Napo and quebradas (0°49′S, 75°31′W). FMNH 102156, 5 specimens, 117.8–158.9 mm; upper Río Tiputini, upstream from bridge (0°44′30″S, 76°53′00″W). USNM 311303, 1 specimen, 58.5 mm; Estero Triniti, 45 min by boat from Rocafuerte on left margin of Río Yasuni. Peru: Loreto: FMNH 111343, 1 specimen, 54.5 mm, Punto Caño, about 7 km above mouth of Río Chambira in Río Maranon (5°0′S, 74°53′W). FMNH 111344, 2 specimens, 40.6–46.4 mm; Río Chambira and small tributaries above mouth in Río Maranon (5°0′S, 74°53′W). FMNH 111608, 1 specimen, 81.3 mm; Río Amazonas drainage, upstream from Iquitos.

Leporinus ortomaculatus Garavello – Venezuela, Amazonas: ANSP 182671, 6 specimens, 54.9–74.2 mm; Río Orinoco, 117 km east of La Esmeralda (03°17′24″N, 66°36′00″W). Bolivar: ANSP 159346, 5 specimens, 50.2–78.0 mm; caño (possibly Caño Curimo) feeding Río Caura near confluence of Río Caura and Río Orinoco (07°37′48″N, 64°50′42″W). ANSP 160346, 2 specimens, 42.0–47.3 mm; confluence of Río Orinoco and Río Caura at Las Piedras (07°38′36″N, 64°50′00″W).

Leporinus sp – Brazil, Rondônia: INPA 15405, 5 specimens, 81.6–115.9 mm; Rio Ucupá ± 5 km above Ji Paraná.